Linear Control of Nonlinear Systems: Interplay between Nonlinearity and Feedback

S. Alper Eker and Michael Nikolaou
Chemical Engineering Dept., University of Houston, Houston, TX 77204

A rigorous and general theory, as well as an associated efficient computational methodology, was developed that addresses the question of when and what linear control is adequate for a nonlinear process. A number of computer simulation examples illustrate the power of the proposed approach. Several potential future developments are outlined.

Introduction

Feedback control of chemical processes that are assumed to behave linearly has a long history of research and successful industrial applications. From single-input-single-output proportional-integral-derivative (SISO PID) controllers to plantwide model-predictive control (MPC) systems (Qin and Badgwell, 1997), feedback control systems that implicitly or explicitly rely on the premise of linear process behavior are to be found in every chemical plant. Underlying this premise are two fundamental assumptions (Slotine and Li, 1991), namely: (a) process dynamics are inherently linear; and/or (b) the controlled process will be operating closely enough to a steady state for its dynamic behavior to be considered approximately linear.

The premise of linear process dynamics is very often useful. Its obvious appeal relies on greatly facilitating a number of control oriented tasks, such as model development, controller design, control system implementation, and maintenance. It has found wide applicability in a number of process industries (Qin and Badgwell, 2000; Nikolaou, 1997). However, there are important instances for which it may be violated, such as:

- regulator-control problems where the process is highly nonlinear and frequently perturbed far from its steady state by large disturbances (such as pH control); and
- servo-control problems where the operating points change frequently and span a sufficiently wide range of nonlinear process dynamics (such as polymer manufacturing and ammonia synthesis).

Correspondence concerning this article should be addressed to M. Nikolaou.

Such instances are not uncommon in chemicals, polymers, natural gas processing, and pulp and paper plants (Qin and Badgwell, 2000); thus, at times necessitating nonlinear control algorithms. As a historical aside, it is interesting to note that an early academic publication, which introduced what today would be called nonlinear MPC, explicitly recognizes and deals with the issue of nonlinearity for model-based control of a distillation column through online optimization (Rafal and Stevens, 1968).

The development, implementation, and maintenance costs of nonlinear control algorithms are usually substantially higher than those of linear control algorithms for the same process. Therefore, before one undertakes the development of a nonlinear control system for a given nonlinear process, one must carefully examine the limits of linear control performance by resolving the following basic question: *For a given process, is linear control adequate or would nonlinear control be necessary?* In the context of the above discussion on control system design and assumptions (a) and (b), the above basic question entails the following questions:

- *How nonlinear are the inherent dynamics of a nonlinear process?*
- *How close to a steady state should a nonlinear process operate to behave almost linearly?*

Attempts to answer the above questions have appeared in literature in recent years, as will be discussed later. Given the many facets in which nonlinearity can manifest itself, it is not surprising that a number of creative approaches, often attacking the problem from widely differing angles, have been proposed by various investigators. Such approaches concentrate on the inherent nonlinearity of the open-loop system

(process and/or controller) over different operating ranges (Nikolaou, 1993; Allgöwer, 1996; Sun and Kosanovich, 1998; Guay, 1996; Stack and Doyle, 1997; Helbig et al., 2000). Various nonlinearity measures and indices have been accordingly proposed, with the intention being to be able to quantify process nonlinearity in terms of a single number. The premise of these approaches is that if a nonlinear open-loop system is "far" from a linear one, then linear control will, most probably, be inadequate for the closed loop. While that may frequently be true, proximity of a nonlinear open-loop system to a linear one is, in general, neither necessary nor sufficient for adequacy of linear control of a nonlinear system. Therefore, this kind of nonlinearity quantification may be helpful for closed-loop *analysis* (because the nonlinearity of the closed-loop can always be quantified using any of the proposed approaches), but may be at best *incomplete* for control system synthesis.

Yet, one would expect that there must be some connection between the nonlinearity magnitude of a process to be controlled and the nonlinearity magnitude of a closed-loop containing a linear controller designed for that process. This expectation, in turn, raises the following questions:

- *How does the nonlinearity magnitude of a process affect the nonlinearity magnitude of the closed loop if a linear controller is to be used?*
- *How does the choice of a linear controller affect the nonlinearity magnitude of the closed loop for a given nonlinear process?*

Answers to the above two questions should provide insight into what are the limits of linear control, rather than just quantifying the nonlinearity of a closed loop for a given linear controller.

To date, both of the above questions have remained rather unresolved. Of course, answers to related control problems that treat nonlinearity as modeling uncertainty have appeared under various guises in the vast literature of robust control theory (for example, Morari and Zafiriou, 1989; Green and Limebeer, 1995; Zhou and Doyle, 1998; Dullerud and Paganini, 2000). Yet, a clear answer to the above two questions is lacking.

In this work, we develop a theory and an associated computational methodology that attack the above basic questions.

The theory is both rigorous and general. It relies on representation of a nonlinear process as an operator that maps input signals to output signals (Eq. 3). As such, the theory is applicable to an extremely wide class of nonlinear processes. Using that theory, the nonlinearity of a closed loop is defined as the distance between a closed loop with nonlinear process/linear controller (Figure 1) and a suitably defined ideal linear closed loop (Definition 1) that reflects control objectives. The basic result of this theory is Theorem 1, which places bounds on closed-loop nonlinearity that depend both on the nonlinearity of the controlled (open-loop stable) process and on a linear controller guaranteed to stabilize the nonlinear process. Computation of these bounds can be performed rigorously using Theorem 2, although the required computations may be complicated. Approximations to these bounds can be computed using a computationally efficient and intuitive approach based on Corollary 3, as described later in the article. More importantly, this approach enables the designer to easily design linear stabilizing controllers with predictable effects on closed-loop nonlinearity (hence, performance) for explicitly characterizable regions of process operation, without having to assume process operation near a steady state. Hence, limits of linear controller performance, as well as the linear controllers that reach these limits, can thus be determined. Process information needed in these computations is multiple linear time-invariant process models, with each model being valid around a steady state within a range of process operation. Thus, the proposed theory and associated computational methodology also create a firm basis and establish novel ways for use of multiple linear models in nonlinear system identification and controller design, an approach that has been repeatedly proposed by several authors (Chen et al., 2000; Johansen and Foss, 1999; Chikkula et al., 1998; Cao et al., 1997; Banerjee et al., 1997, among others) on the basis of intuitive arguments.

In the sequel, a number of motivating examples are provided. A very brief overview is provided of the nonlinear operator analysis framework used in this work, as well as a succinct review of previous efforts on nonlinearity quantification that are relevant to this work. The main results are presented. A number of examples are shown that demonstrate how our results can be used in practice to resolve questions such as those raised by the motivating examples in the second section. Results are summarized, put into perspective, many questions that are still open are identified, and promising directions for future work are proposed.

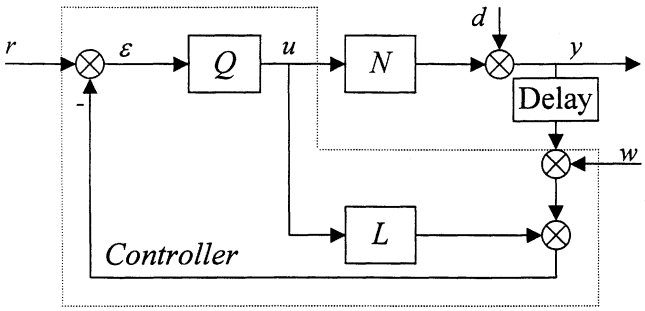

Figure 1. IMC for an nonlinear process *N*.

Motivating Examples

The following motivating examples raise a number of questions and set the stage for the development of the theory and methodology presented later. Details on these examples and resolution of the questions raised in this section are provided in the Examples section.

Motivating Example 1

Consider the exothermic reaction $A \rightarrow B$ in a system of two jacket-cooled continuous stirred-tank reactors (CSTR) in series (Henson and Seborg, 1990), as described in Example 1 of the subsequent section. The concentration of the reactant at the exit of the second CSTR C_{A2} is the controlled variable, and the coolant flow rate q_c (common for both reactors) is the manipulated variable. The dashed line in Figure 2 shows

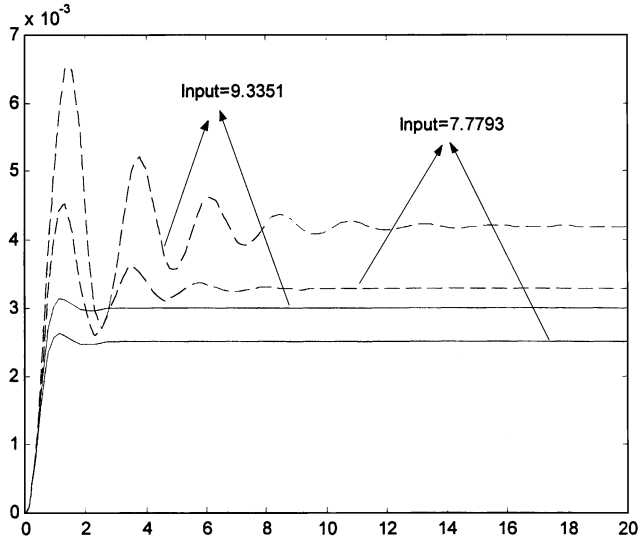

Figure 2. Open-loop responses of the nonlinear CSTR of Example 2 (dashed lines) and its linearization around the nominal steady state of Table 1 (solid lines) for input step changes of +9.3351 and +7.7793.

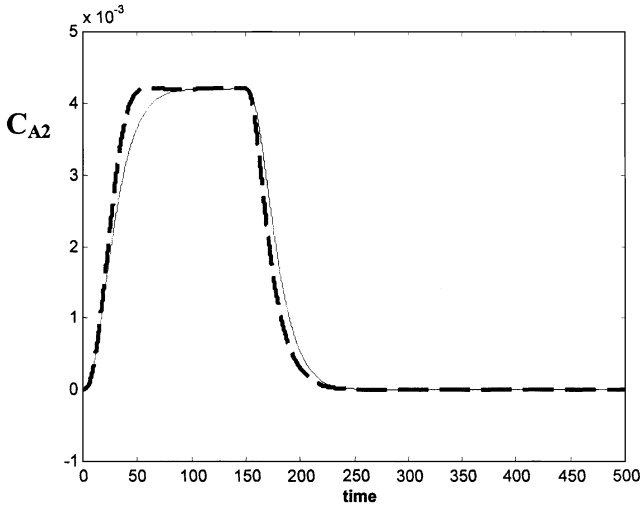

Figure 3. Closed-loop responses: (a) nonlinear process (Eqs. 55–58) with the designed IMC controller ($\lambda = 10$); (b) linearized system, Eq. 59, with the same IMC controller (perfect model assumption) for pulse set point change of amplitude $+4.2\times10^{-3}$ mol/L.

the response of C_{A2} (in deviation from its steady-state value of $C_{A2s} = 5.3\times10^{-3}$ mol/L) resulting from a step change in the input. C_{A2} eventually deviates from its steady-state value by 80%. When the linearization of this system around the above steady state is subjected to the same step change in the input, the output corresponding to the solid line in Figure 2 results. The system appears to be fairly nonlinear.

When the linear internal-model control (IMC) with the IMC-filter time-constant $\lambda = 10$ (Eq. 40) (Morari and Zafiriou, 1989, p. 65) is used to effect a pulse set point change of $+4.2\times10^{-3}$ mol/L (+80% of the steady-state value) on C_{A2}, we get the closed-loop responses of Figure 3, where the dashed line corresponds to the actual output of the nonlinear closed loop, while the solid line corresponds to the closed-loop output that would be obtained if the plant were linear. Figure 4 depicts the same situation when the IMC-filter time-constant is $\lambda = 1$. It is clear that the closed-loop response is virtually linear when $\lambda = 1$, even though the open-loop system is fairly nonlinear when the output is steered to the same final value.

- *How does feedback alter nonlinearity?*
- *By how much?*
- *Is the decrease of closed-loop nonlinearity universal for decreasing values of the IMC-filter time constant λ?*
- *How small could λ be made without jeopardizing closed-loop stability?*

Motivating Example 2

Continuing on Example 1, Figure 5 shows the closed-loop response of C_{A2} for a pulse set point change of $+5.2\times10^{-3}$ mol/L (+100% of the steady-state value) when $\lambda = 1$. It is clear that the actual nonlinear response (dashed line) is far from the ideal linear response (solid line) after approximately time 70.

- *Why is Figure 5 so different from Figure 4?*
- *What set point changes would not create large discrepancies between the actual nonlinear closed-loop behavior and the ideal linear behavior?*
- *How would such set point changes depend on the choice of linear feedback controller?*
- *Would phenomena similar to those in Figure 5 appear in Figure 4 if the pulse of Figure 4 lasted much longer?*

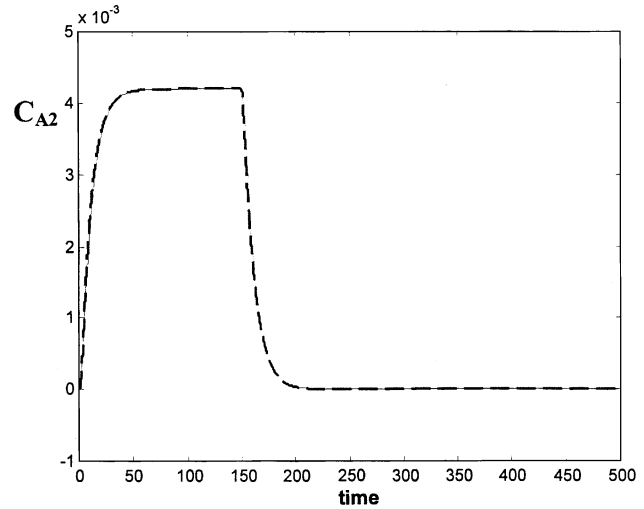

Figure 4. Closed-loop responses: (a) nonlinear process (Eqs. 55–58) with the designed IMC controller ($\lambda = 1$); (b) linearized system (Eq. 59), with the same IMC controller (perfect model assumption) for pulse set point change of amplitude $+4.2\times10^{-3}$ mol/L.

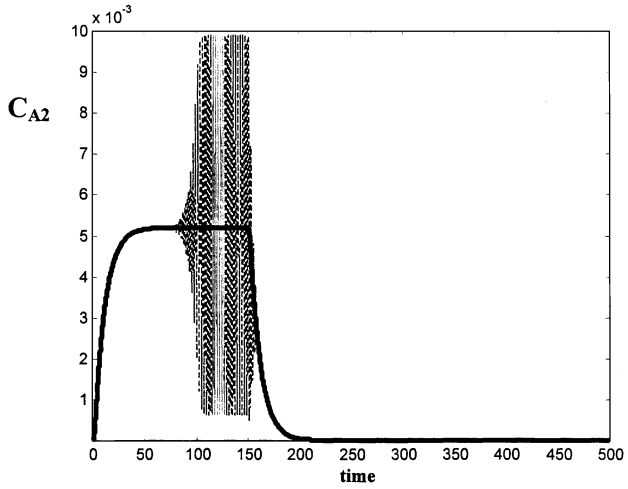

Figure 5. Closed-loop responses: (a) nonlinear process (Eqs. 55–58) with the designed IMC controller ($\lambda = 1$); (b) linearized system (Eq. 59), with the same IMC controller (perfect model assumption) for pulse set point change of amplitude $+5.2 \times 10^{-3}$ mol/L.

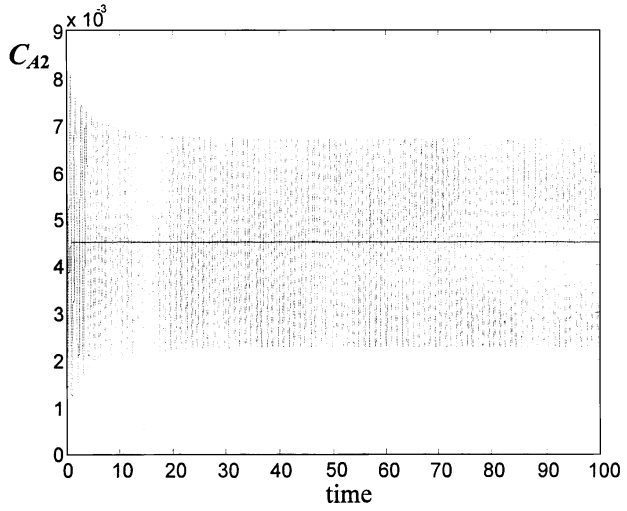

Figure 7. Response: (a) nonlinear closed loop with linear IMC and $\lambda = 0.1$ (dashed line); (b) ideal linear closed loop with the same IMC (solid line) to set point step change of magnitude $+4.5 \times 10^{-3}$.

Measurement is delayed by 5 time units (Example 3).

Motivating Example 3

In Example 3, the system of Example 1 is considered, with the addition of time delay to actual output measurements. Such delay may be inherent, for example, due to the presence of an online composition analyzer. The control designer designs a linear IMC controller for the linearized model of the nonlinear process, without taking the measurement delay into account. Figure 6 shows how C_{A2} would respond to a set point step change if the plant were linear, there was a measurement delay of 5 time units, and the above linear IMC controller with $\lambda = 0.1$ was used. The design appears to be fairly robust to the presence of measurement delay. However, when the same controller is applied to the actual nonlinear system with the same measurement delay, very unsatisfactory (unstable) response results, as seen in Figure 7. Retuning the IMC controller to $\lambda = 10$ appears to solve the robustness problem, as seen in Figure 8.

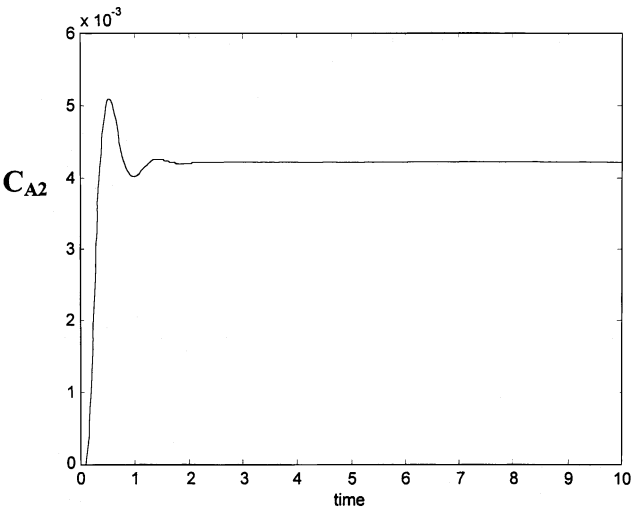

Figure 6. Response of a linear closed loop, with linear process *L*, measurement delay of 5, and linear IMC employing a model *L* and filter *F* with $\lambda = 0.1$ to set point change of $+4.2 \times 10^{-3}$ (Example 3).

- *Given that overly aggressive IMC tuning is known to compromise closed-loop robustness, how, exactly, does the linear IMC design work for Figure 8 and fail for Figure 7?*
- *How could robustness considerations be explicitly incorporated into the linear controller synthesis for nonlinear processes?*

Motivating Example 4

Consider the irreversible exothermic reaction $A \rightarrow B$ in a CSTR, as discussed in Example 4 below. The controlled output is the concentration of the reactant A in the effluent, C_A, and the manipulated input is the feed flow rate. The CSTR has inverse-response dynamics. Figure 9 shows the closed-loop responses of C_A to step-changes in the set point, when IMC based on a linear CSTR model is used with (a) the actual nonlinear CSTR (dashed line), and (b) the CSTR's hypothetical linearized model (solid line). The actual closed-loop response is clearly problematic, even though the ideal linear response is good.

- *Could this closed-loop behavior have been predicted?*
- *Is it possible to design a linear controller that avoids such problems in a systematic way?*
- *Is it possible to make the closed-loop behavior of this CSTR almost linear using a linear controller?*

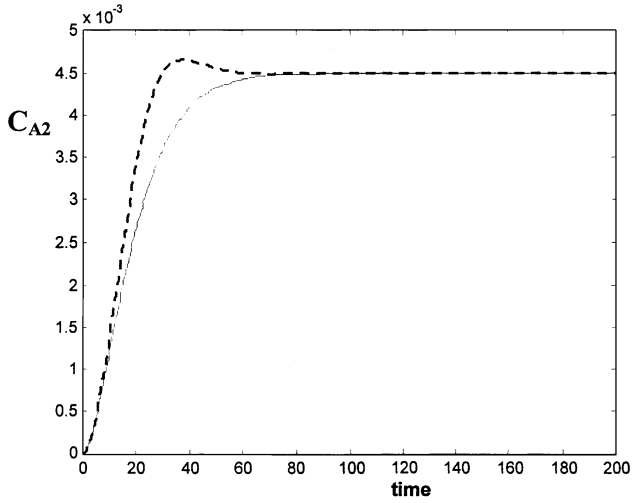

Figure 8. Response: (a) nonlinear closed loop with linear IMC and $\lambda = 10$ (dashed line); (b) ideal linear loop with the same IMC (solid line) to set point step change of magnitude $+4.5 \times 10^{-3}$.

Measurement is delayed by 5 time units (Example 3).

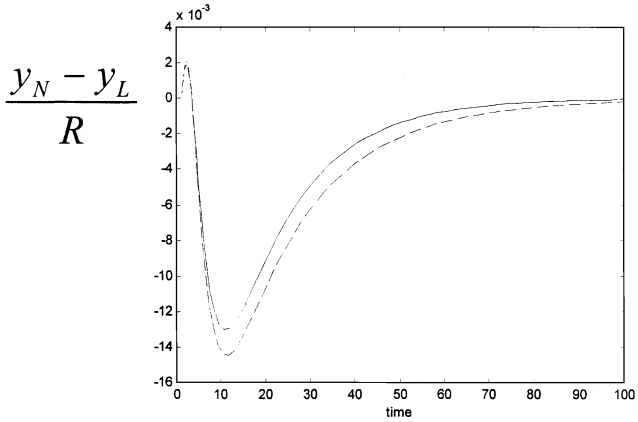

Figure 10. Scaled difference $(y_N\text{-}y_L)/R$ between the response of the nonlinear closed loop y_N and the ideal linear closed loop y_L to set point changes R of magnitudes 0.0145 (solid line) and 0.0158 (dashed line).

Both loops contain the same linear IMC controller with $\lambda = 1$ (van de Vusse CSTR, Example 6).

Motivating Example 5

Consider a CSTR with a van de Vusse type of reaction scheme, as discussed in Example 5 below. Van de Vusse reaction systems are well known to be "strongly nonlinear." For this CSTR, the concentration of the product B in the effluent is the controlled variable, and the flow rate through the reactor is the manipulated variable. A linear IMC controller is designed using a linear model around a given nondegenerate steady state. Two different values for the IMC-filter parameter λ are considered: $\lambda = 1$ and $\lambda = 10$. Step changes in the set point are performed. Figure 10 ($\lambda = 1$) and Figure 11 ($\lambda = 10$) show the discrepancies between (a) closed-loop responses of the actual (nonlinear) CSTR output under the above linear IMC, and (b) closed-loop responses of the output that would be obtained if the CSTR behaved exactly like the linear model employed by the above linear IMC. Figure 10 and Figure 11 clearly show that increasing the value of the time constant λ of the linear IMC filter from 1 to 10 results in considerably *increased* peak discrepancy between the outputs of the actual nonlinear and the ideal linear closed-loop.

However, similar experiments with the CSTRs of Example 1 and Example 4 show the exact opposite behavior, namely increasing the value of the time constant λ of the linear IMC filter results in considerably *decreased* peak discrepancy between the outputs of the actual nonlinear closed-loop and the ideal linear closed-loop, as shown by comparing Figure 12 with Figure 13 (Example 4) and Figure 14 with Figure 15 (Example 1).

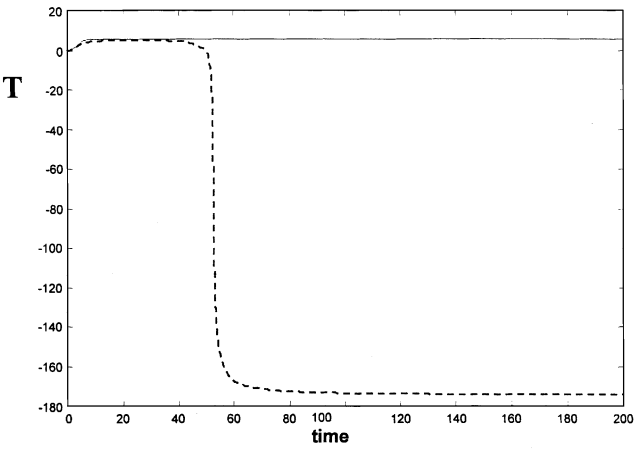

Figure 9. Step responses of ideal linear (solid line) and nonlinear (dashed line) closed-loops with linear IMC ($\lambda = 1$) to set point change +5.5 (Example 4).

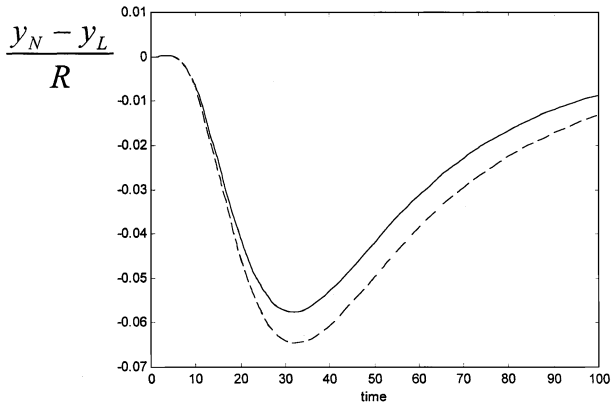

Figure 11. Scaled difference $(y_N\text{-}y_L)/R$ between the response of the nonlinear closed loop y_N and the ideal linear closed loop y_L to set point changes R of magnitudes 0.0145 (solid line) and 0.0158 (dashed line).

Both loops contain the same linear IMC controller with $\lambda = 10$ (van de Vusse CSTR, Example 6).

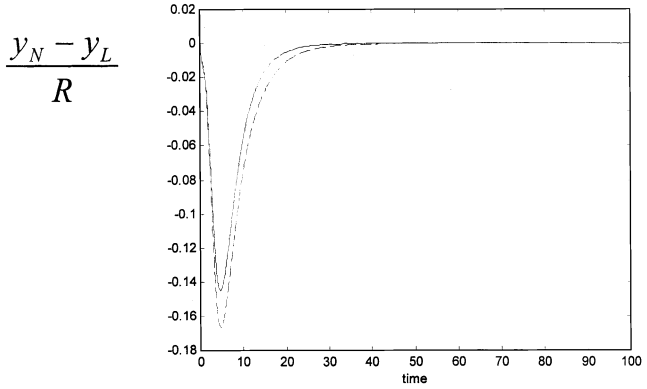

Figure 12. Scaled difference $(y_N\text{-}y_L)/R$ between the response of the nonlinear closed loop y_N and the ideal linear closed loop y_L to set point changes R of magnitudes 3.74 (solid line) and 4.29 (dashed line).

Both loops contain the same linear IMC controller with $\lambda = 1$ (CSTR with unstable inverse, Example 6).

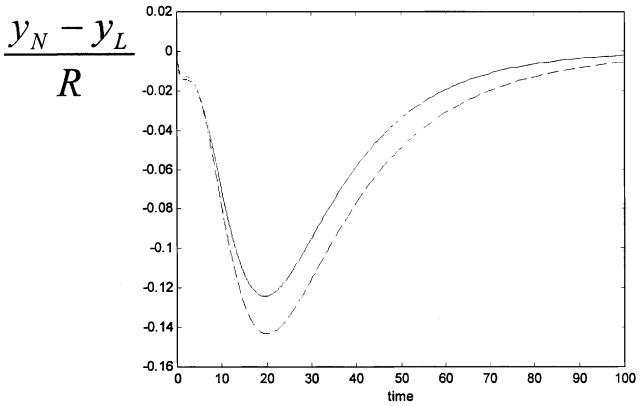

Figure 13. Scaled difference $(y_N\text{-}y_L)/R$ between the response of the nonlinear closed loop y_N and the ideal linear closed loop y_L to set point changes R of magnitudes 3.74 (solid line) and 4.29 (dashed line).

Both loops contain the same linear IMC controller with $\lambda = 5$ (CSTR with unstable inverse, Example 6).

- *How could the above different closed-loop nonlinearity trends be rigorously explained?*
- *In general, should the time-constant λ of a linear IMC filter take large or small values?*
- *Within what limits should λ take values?*
- *How could the effect of linear IMC tuning on closed-loop nonlinearity be rigorously predicted, so that linear IMC controllers for nonlinear systems can be synthesized?*

Background

Nonlinear operator analysis

Basics of the input-output system framework can be found in Willems (1971) and Desoer and Vidyasagar (1975). Within this framework, the magnitude of a signal $x{:}[0,\infty) \rightarrow \Re^n$ is quantified through its p-norm ($p \geq 1$), defined as

$$\|x\|_p \triangleq \begin{cases} \left[\int_{S \subset \Re} \|x(t)\|^p dt \right]^{1/p} & \text{if } p \in [1,\infty) \\ \underset{t \in [0,\infty)}{ess\ \sup} \|x(t)\| & \text{if } p = \infty \end{cases} \quad (1)$$

where $\|x(t)\|$ denotes any norm of the vector $x(t) \in \Re^n$. Signals with finite p-norms form a (Banach) space L_p^n, defined as

$$L_p^n \triangleq \{x{:}[0,\infty) \rightarrow \Re^n{:}\ \|x\|_p < \infty\} \quad (2)$$

The dynamic behavior of a nonlinear system is described by an unbiased nonlinear operator (mapping)

$$N{:}U \rightarrow Y{:}u \mapsto y = Nu{:}0 \mapsto N(0) = 0 \quad (3)$$

which maps input signals u in the space U to output signals y in the space Y. Note that there is no unanimity in literature regarding uniqueness of y given u. We will not assume uniqueness in this work.

The operator N is commonly realized through a set of ordinary or partial differential equations and algebraic equations, such as

$$\frac{dx}{dt}(t) = f[x(t),u(t)], \quad y(t) = h[x(t),u(t)] \quad (4)$$

subject to initial or boundary conditions.

The norm and incremental norm (gain and incremental gain or local Lipschitz constant) of $N{:}U \rightarrow Y$ over the set $V \subseteq U$

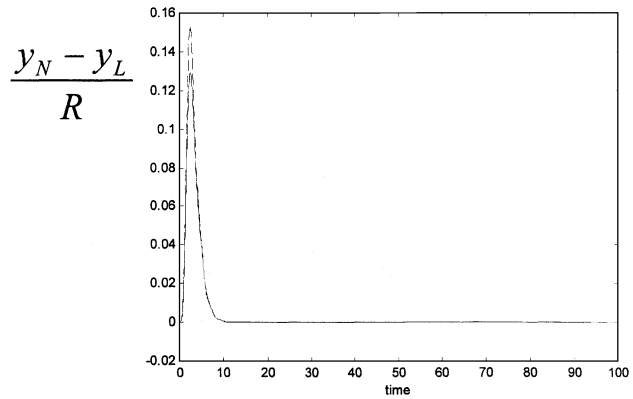

Figure 14. Scaled difference $(y_N\text{-}y_L)/R$ between the response of the nonlinear closed loop y_N and the ideal linear closed loop y_L to set point changes R of magnitudes 0.0025 (solid line) and 0.0029 (dashed line).

Both loops contain the same linear IMC controller with $\lambda = 1$ (two CSTRs in series, Example 6).

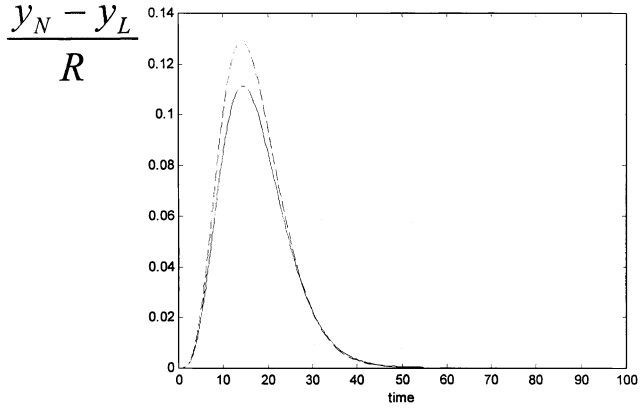

Figure 15. Scaled difference $(y_N\text{-}y_L)/R$ between the response of the nonlinear closed loop y_N and the ideal linear closed loop y_L to set point changes R of magnitudes 0.0025 (solid line) and 0.0029 (dashed line).

Both loops contain the same linear IMC controller with $\lambda = 5$ (two CSTRs in series, Example 6).

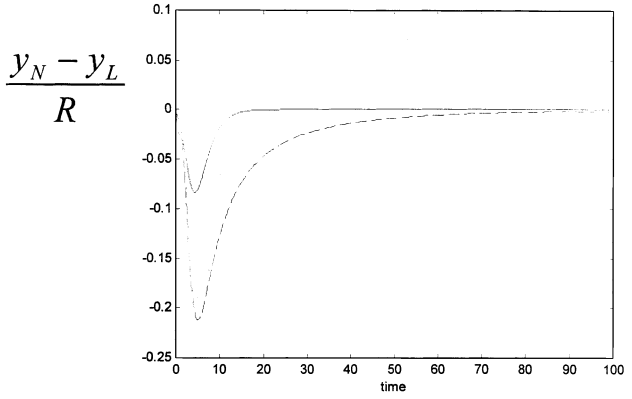

Figure 17. Scaled difference $(y_N\text{-}y_L)/R$ between the response of the nonlinear closed loop y_N and the ideal linear closed loop y_L to set point changes R of magnitudes 2.09 (solid line) and 5.39 (dashed line).

Both loops contain the same linear IMC controller with $\lambda = 1$ (Example 4).

are defined (Nikolaou and Manousiouthakis, 1989) as

$$\| N \|_V = \sup_{\substack{u \in V \\ u \neq 0}} \frac{\| Nu \|}{\| u \|} \tag{5}$$

and

$$\| N \|_{\Delta V} = \sup_{\substack{u_1, u_2 \in V \\ u_1 \neq u_2}} \frac{\| Nu_1 - Nu_2 \|}{\| u_1 - u_2 \|} \tag{6}$$

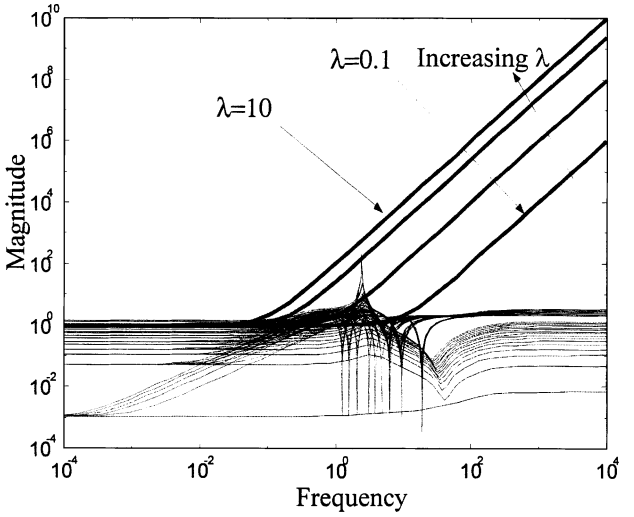

Figure 16. Bode plots of (a) $1/|G_F(j\omega)|$ (Thick lines) for various values of λ, and (b) $|[G_{L_{u_i}}(j\omega)\text{-}G_L(j\omega)]/[G_L(j\omega)]|$ for different u_i, both without delay in $G_{L_{u_i}}(j\omega)$ (solid lines) and with delay approximated by 5th-order Padé approximation (dashed lines).

respectively, where the norm functions on the righthand sides of Eqs. 5 and 6 are defined on the spaces U and Y. The set V identifies these input signals that are physically important for the operator N, such as mole fractions in [0,1]. An operator $N{:}U \to Y$ is bounded (stable) over the set V when

$$\| N \|_{\Delta V} < \infty. \tag{7}$$

Note that the above definition of stability supercedes the standard stability definition $\| N \|_V < \infty$, because $\| N \|_V \leq \| N \|_{\Delta V}$. Note also that even for very simple nonlinear operators it is possible to have $\| N \|_{\Delta V_1} = \infty$ and $\| N \|_{\Delta V_2} < \infty$ (or $\| N \|_{V_1} = \infty$ and $\| N \|_{V_2} < \infty$) for two different sets V_1 and V_2 (Nikolaou and Manousiouthakis, 1989).

The linearization of an operator $N{:}U \to Y$ around the input trajectory u_0 is defined as the linear operator $L_{u_0}{:}U \to Y$

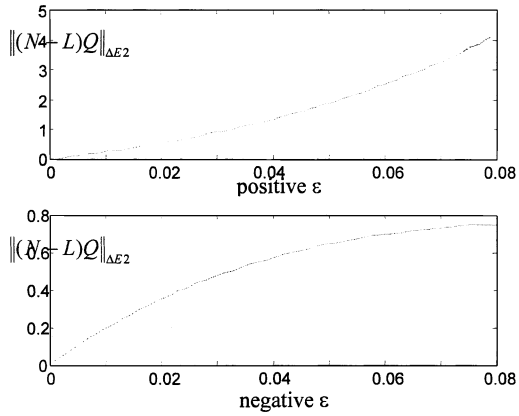

Figure 18. Incremental norm with different sign of input change for different filter coefficients $\lambda =$ 1,10,100 (Example 5).

satisfying the equation

$$\lim_{u \to 0} \frac{\| N(u_0 + u) - Nu_0 - L_{u_0} u \|}{\| u \|} = 0$$

For an operator defined via Eq. 4, the linearization of N is a linear time-varying operator, defined by the equations

$$\frac{d\Delta x}{dt}(t) = \frac{\partial f}{\partial x}\big[x_0(t), u_0(t)\big]\Delta x(t) + \frac{\partial f}{\partial u}\big[x_0(t), u_0(t)\big]u(t)$$

$$y(t) = \frac{\partial h}{\partial x}\big[x_0(t), u_0(t)\big]\Delta x(t) + \frac{\partial h}{\partial u}\big[x_o(t), u_0(t)\big]u(t) \quad (8)$$

where $x_0(t)$ is the solution of Eq. 4 corresponding to $u_0(t)$ and $\Delta x(0) = 0$.

For a cascade of operators $N = N_1 N_2$, the linearization of N around u_0 can be shown to be equal to the cascade of linearizations as

$$L^N_{u_0} = L^{N_1}_{N_2 u_0} L^{N_2}_{u_0} \quad (9)$$

As a corollary, the linearization of the inverse of an operator is equal to the inverse of its linearization as

$$L^{N^{-1}}_{Nu_0} = \left(L^N_{u_0}\right)^{-1} \quad (10)$$

Nonlinearity quantification

For a meaningful quantification of the nonlinearity measure of a nonlinear system, one must explicitly state what is the intended purpose of such quantification. The performance of a linear feedback controller designed for a forced nonlinear system is the focus of this work.

In that context, efforts have appeared in literature to quantify the nonlinearity of an operator by computing its distance from a suitably defined linear operator.

Desoer and Wang (1980) defined the nonlinearity measure of a nonlinear operator N as

$$\upsilon \triangleq \inf_{L \epsilon \Lambda} \| N - L \| \quad (11)$$

where the above minimization is performed over all linear operators L in the set Λ, and the norm function can be any suitable norm. Desoer and Wang (1980) were not concerned with the computation of υ, but rather with its definition. However, if one uses an induced norm, such as Eq. 5 in Eq. 11, then the computation of υ becomes extremely complicated.

To address computational issues in the computation of υ as defined in the above Eq. 11, Nikolaou (1993) constructed an inner product and corresponding norm theory for nonlinear operators. Based on that theory, υ, corresponding to the average discrepancy between outputs of N and L for inputs within an explicitly specified set, can be trivially computed via Monte Carlo simulations. In addition, explicit formulas for the optimal L in Eq. 11 can be derived. Using this theory, Nikolaou and Hanagandi (1998) quantified the nonlinearity of several chemical engineering systems, and showed that polynomial nonlinearities, usually thought of as mild, may be severe, and exponential nonlinearities, usually thought to be severe, may be mild, according to both the system at hand and how far from a steady state the system operates. The same authors also showed how the nonlinearity of a system may vary from mild to severe according to the magnitude of the system's inputs, demonstrated quantitatively how a feedback loop may exhibit much lower nonlinearity than an open-loop nonlinear system, and showed how different tunings of a linear IMC controller used to control a nonlinear process may result in closed loops of significantly different nonlinearity magnitudes.

While computationally efficient for the analysis of open- or closed-loop systems, the approach introduced by Nikolaou (1993) has the shortcoming that the norm employed in Eq. 11 is not an induced norm; therefore, it does not satisfy the submultiplicativity property ($\| N_1 N_2 \| \leq \| N_1 \| \| N_2 \|$), thus making it difficult to use in direct feedback controller synthesis.

Allgöwer (1996) tackled the problem of using an induced norm (Eq. 5) with Eq. 11, by parametrizing the input signal u in Eq. 5 and the linear operator L in Eq. 11 through finite-dimensional approximations and directly performing the optimization

$$\upsilon = \inf_{L \in \Lambda} \sup_{\substack{u \in V \\ u \neq 0}} \frac{\| Nu - Lu \|}{\| u \|} \quad (12)$$

For a number of examples, he found that the value of υ is insensitive to the particular parametrization of u. The nonlinearity measure computed via Eq. 12 corresponds to the worst possible discrepancy between outputs of N and L.

Helbig et al. (2000) defined a nonlinearity measure as

$$\phi = \inf_{L \in \Lambda} \sup_{\substack{u \in U \\ x_{N,0} \in X_{N,0}}} \inf_{x_{L,0} \in X_{L,0}} \frac{\| N[u, x_{N,0}] - L[u, x_{L,0}] \|}{\| N[u, x_{N,0}] \|} \quad (13)$$

This measure focuses on the discrepancy of output of N and L as a function of both initial conditions and inputs. It takes values between 0 and 1, thus allowing easy nonlinearity assessment for a value of ϕ. Computing ϕ is practically infeasible. However, Helbig et al. (2000) have shown how to efficiently calculate good approximations or bounds of ϕ by finite-dimensional parametrization of u and convex optimization.

To avoid having to directly optimize with respect to L in nonlinearity measures such as in Eqs. 11 through 13, Sun and Kosanovich (1998) proposed to quantify nonlinearity as

$$\max\left\{ \sup_{u \in U} \| Nu - L_{\text{upper}} u \|, \sup_{u \in U} \| Nu - L_{\text{lower}} u \| \right\} \quad (14)$$

where L_{upper} and L_{lower} are linear operators such that they provide the smallest bounding envelope on the output of N as $(L_{\text{lower}}u)(t) \le (Nu)(t) \le (L_{\text{upper}}u)(t)$ for $u \in U$. This approach has many similarities to identification for robust control proposed by Helmicki et al. (1991, 1992).

In all of the above approaches the focus is on assessing the nonlinearity of a given system, whether that would be the controlled process in open loop or the entire closed-loop involving a nonlinear process and a linear controller. In an effort to better assess the need for nonlinear control, as opposed to just assessing the distance of nonlinear plant from a linear one, Stack and Doyle (1997) proposed to focus on the nonlinearity magnitude of an optimal *nonlinear controller* designed for a nonlinear process. Quantification of the nonlinearity of that controller, using any method, was proposed by these authors as a measure of the need for nonlinear control, the assumption being that a highly nonlinear controller would result in a highly nonlinear closed loop, hence, rendering linear control inadequate and necessitating nonlinear control. For static state feedback laws, these authors proposed to use coherence analysis as the nonlinearity measure. However, the optimal nonlinear control structure proposed was based on determination of an open-loop optimal input profile over a horizon, whereas a feedback control law would require the dependence of the value of the process input as a function of state measurement at the first time point of a moving horizon. It might also be argued that if the optimal nonlinear control structure for a given process were known, then that structure, rather than a linear one, might actually be used.

Stack and Doyle (1999) also applied coherence analysis to the assessment of closed-loop nonlinearity for a nonlinear system controlled by linear IMC. Emphasis was placed on the effect of different IMC tunings on closed-loop nonlinearity. An advantage of coherence analysis is that its entailed computational load is trivial, and the analysis may be conducted using experimental data, without detailed knowledge of a process model. This may be of great practical significance.

Departing from the notion of nonlinearity measures based on the distance of a nonlinear operator from a suitable linear operator, Guay et al. (1995) proposed to quantify the static nonlinearity of a system described by Eq. 4 in terms of the local geometry of the steady-state locus, that is, by considering the first and second derivatives of the steady-state map $0 = f(x_s,u_s)$ with respect to u_s. Guay (1996) extended these results to quantification of dynamic nonlinearity.

The premise of the above approaches is that, if a nonlinear process is "close" to a linear one, then a linear controller will be sufficient and vice versa. While that may frequently be true, the proximity of a nonlinear process to a linear one is neither necessary nor sufficient for good closed-loop performance. For example, Nikolaou and Hanagandi (1998) have shown that a highly nonlinear process controlled by linear IMC may result in an almost linear closed loop, if IMC is suitably designed. Conversely, Schrama (1992) has shown that, even for a linear process, a controller design based on a linear model with close proximity to a process may even result in closed-loop instability. Nevertheless, one would intuitively expect that there must be controller-dependent connections between open- and closed-loop nonlinearity. That intuition is indeed correct, as shown in the following section.

Results

Basic lemmas and definitions

In this subsection we prove basic lemmas that we will use to prove the main results of the following subsections.

Lemma 1: Invertibility and Boundedness (Stability) of a Nonlinear Operator T over a Set. Consider the nonlinear operator $T:U \to X$, where U, the domain set, and $X = T(U)$, the image set, are subsets of normed spaces. Then, the following two statements are equivalent:

(1) There exists a constant $c > 0$ such that

$$\|Tu_1 - Tu_2\| \ge c\|u_1 - u_2\| \ \forall u_1,u_2 \in U \tag{15}$$

(2) The inverse of T, $T^{-1}:X \to U$, exists on X, and T is bounded (stable) over the set X with

$$\|T^{-1}\|_{\Delta X} \le \frac{1}{c} < \infty \tag{16}$$

Proof. See Appendix A.

Remark 1: Scope of Lemma 1. Note that Tu need not be uniquely defined! Output multiplicities (the same input is mapped to more than one output) are allowed for the operator T (such as $Tu \triangleq \pm\sqrt{u}$, $0 < u \le u_{\max}$).

Lemma 2: Existence and Boundedness (Stability) of the Operator $(I + R)^{-1}$ over a Set. Consider the nonlinear operator $(I + R):U \to Y$, where I is the identity operator, U is the domain set, and $Y = (I + R)(U)$ is the image set, and both U and Y are subsets of normed spaces. Let

$$\|R\|_{\Delta U} < 1 \tag{17}$$

for an incremental norm over U. Then, the inverse of $I + R$, $(I + R)^{-1}:Y \to U$, exists on Y and is bounded as

$$\left\|(I + R)^{-1}\right\|_{\Delta Y} \le \frac{1}{1 - \|R\|_{\Delta U}} \tag{18}$$

Proof: See Appendix B.

Remark 2: Importance of Lemma 2. (1) Results similar to Lemma 2 are well known in mathematical systems literature (for example, Willems, 1971) as variants of Banach's contraction mapping theorem (Saaty and Bram, 1964, p. 37; Saaty, 1967, p. 34; Shinbroth, 1966). However, there is a small but crucial difference between Lemma 2 and standard literature results: Lemma 2 is proven for the sets U and Y not being entire Banach spaces. This is extremely important when dealing with feedback control systems, because the behavior of such systems may vary drastically when different sets of inputs are considered, as shown in the sequel.

(2) Note also that, unlike the case where R is linear, Eq. 17 in Lemma 2 is a sufficient but not necessary condition for the invertibility of $I + R$.

Lemma 3: Closed-Loop Operator for Nonlinear Internal Model Control (IMC) Structure. Consider the IMC loop of Figure 1. The operator N corresponding to the plant is nonlinear, the operator L corresponds to the plant model, and the operator Q is the Youla parameter of the controller. Assume that the closed loop is well posed, that is, $(I + NQ - LQ)^{-1}$ exists. Then

$$y = d + NQ(I + NQ - LQ)^{-1}(r - w - d) \tag{19}$$

Proof. See Appendix C.

Corollary 1: Closed-Loop Operator for Nonlinear IMC Regulator and Servo Problems. When there is no set point change and no noise in Figure 1 ($r = w = 0$), Eq. 19 becomes

$$y = -(I - LQ)(I + NQ - LQ)^{-1}(-d) \triangleq -N_{dy}(-d). \tag{20}$$

When there is no external disturbance in Figure 1 ($d = 0$), Eq. 19 becomes

$$y = NQ(I + NQ - LQ)^{-1}(r - w) \triangleq N_{ry}(r - w). \tag{21}$$

Proof. Straightforward. See Appendix D.

Remark 3: Subtleties in calculations with nonlinear operators. (1) Note that, in general, $-N_{dy}(-d) \neq N_{dy}d$ in Eq. 20 because the operator N_{dy} is nonlinear. Note also that for nonlinear operators A, B, C left-distributivity holds, that is, $(A + B)C = AC + BC$ but right-distributivity does not, that is, in general, $C(A + B) \neq CA + CB$ (Willems, 1971, p. 16). Therefore, $NQ - LQ = (N - L)Q$, regardless of linearity of N, L, or Q.

(2) Note that no linearity assumptions have been made yet about L and Q in the above results.

Control-relevant quantification of closed-loop nonlinearity

If a *linear* IMC controller with *linear* Youla parameter Q based on the stable *linear* model L is used to control the stable *linear* plant L, it is well known that the closed loop is stable if and only if the controller Q is stable (Morari and Zafiriou, 1989). However, if that linear controller is used to control the nonlinear plant N, then the actual closed loop will differ from the nominal (linear) closed loop, and actual performance will be inferior, to a degree that may vary from negligible to severe. It is, therefore, natural to ask the following questions: (a) What is the effect of the nonlinearity of the plant N on closed-loop nonlinearity? (b) What is the effect of the design of the controller Youla parameter Q on closed-loop nonlinearity?

We provide answers to the above questions next.

If the actual plant were stable, linear, and equal to L, then the hypothetical closed-loop operator for the IMC configuration of Figure 1 would produce a plant output y' such that

$$y' = (I - LQ)d + LQ(r - w) = d + LQ(r - w - d) \tag{22}$$

Equations 22 and 19 imply that

$$y - y' = \left[NQ(I + NQ - LQ)^{-1} - LQ\right](r - w - d) = \triangleq \Delta N(r - w - d) \tag{23}$$

where the operator

$$\Delta N \triangleq NQ(I + NQ - LQ)^{-1} - LQ \tag{24}$$

refers to the discrepancy between the nonlinear and hypothetical linear closed loop. To quantify that discrepancy, we propose to use the concept of the *incremental norm over a set* (local Lipschitz constant) as follows.

Definition 1: Control-Relevant Quantification of Closed-Loop Nonlinearity. Let the linear operator W correspond to a stable linear low-pass filter, and let the linear model L and Youla parameter Q of the controller (Figure 1) be linear. Then, the nonlinearity of the closed loop in Figure 1 over the set Z is quantified as

$$\boxed{\|W\Delta N\|_{\Delta Z} \triangleq \left\|W\left(NQ(I + NQ - LQ)^{-1} - LQ\right)\right\|_{\Delta Z}} \tag{25}$$

Remark 4: Why Incremental Norms over Sets for Quantification of Nonlinearity? Definition 1 departs markedly from nonlinearity quantifiers that have appeared in literature, which rely on the norm (instead of the incremental norm) of the difference between a nonlinear operator and a suitable linear operator. There are two reasons for introducing Definition 1:

(a) The incremental norm $\|W\Delta N\|_{\Delta Z}$ over the set Z captures nonlinearity better than the standard norm $\|W\Delta N\|_Z$ over the set Z. Indeed, by definition, $\|W\Delta N\|_Z$ is the least upper bound of the gain experienced by an input signal (in deviation form with respect to its steady-state value) when going through the unbiased operator $W\Delta N$. However, the closed loop may operate far from its original steady state (it may operate around new steady states, or it may be in long transient, responding to ever changing set points or large disturbances). It is clear that incremental changes of the output of $W\Delta N$ corresponding to incremental changes of the input to $W\Delta N$ are far more relevant to quantifying the nonlinearity of the closed loop.

(b) As will be shown below, computations with incremental norms are a lot easier than computations with norms. In addition, powerful closed-loop stability, performance, and robustness results may be obtained using incremental norms, as shown in the sequel.

Lemma 4: Representation of ΔN as a Cascade of Operators. The operator ΔN defined in Eq. 24 with L, Q being linear,

satisfies the equality

$$\Delta N = (I - LQ)(NQ - LQ)(I + NQ - LQ)^{-1}. \quad (26)$$

Proof. See Appendix E.

Remark 5: Generalization of Lemma 4. Note that Lemma 4 is also true under the weaker assumption that the composition LQ of the operators L and Q is linear, rather than each of L and Q being linear.

When the plant N and its linear model L have stable inverses, then the above Definition 1 can be extended in an important way that provides additional insight to the above quantification of closed-loop nonlinearity. To realize this, consider a nonlinear plant N, such that N^{-1} and L^{-1} exist and are stable. For this plant, consider the following two model-based feedback controllers and corresponding closed loops:

(a) A *linear* IMC controller with linear model L and linear Youla parameter $Q_L = L^{-1}F \Leftrightarrow LQ_L = F$ (Figure 1), where the filter F is linear. Then, by Lemma 3 we obtain that the plant output for the closed loop is

$$y_{\text{LinearControl}} = d + NL^{-1}F(I + NL^{-1}F - F)^{-1}(r - w - d) \quad (27)$$

that is, use of *linear* control makes the closed-loop operator $(r,w,d) \mid \rightarrow y_{\text{LinearControl}}$ *nonlinear*.

(b) An optimal *nonlinear* IMC controller with nonlinear model N (in place of L in Figure 1) and nonlinear Youla parameter $Q_N = N^{-1}F \Leftrightarrow NQ_N = F$, where the filter F is the same as in Q_L. Then, by Lemma 3 we obtain that the plant output for the closed loop is

$$y_{\text{NonlinearControl}} = d + F(r - w - d) \quad (28)$$

that is, use of *nonlinear* control makes the closed-loop operator $(r,w,d) \mapsto y_{\text{NonlinearControl}}$ *linear*.

The discrepancy between the closed-loop plant outputs y_L and y_N, corresponding to linear and nonlinear IMC, respectively, is

$$y_{\text{LinearControl}} - y_{\text{NonlinearControl}} = \left[NL^{-1}F(I + NL^{-1}F - F)^{-1} - F \right](r - w - d) \quad (29)$$

The magnitude of the above operator

$$\Delta M \triangleq NL^{-1}F(I + NL^{-1}F - F)^{-1} - F \quad (30)$$

can be used in conjunction with Definition 1 to extend Definition 1 in the following important way.

Definition 2: Comparing a Closed Loop with Linear Control to a Closed Loop with Optimal Nonlinear Control for Plants with Stable Inverses. Let the linear operator W correspond to a stable linear low-pass filter, and let the plant N and linear model L in Figure 1 as well as N^{-1} and L^{-1} be stable. Then, the nonlinearity of the closed loop in Figure 1 over the set Z can be quantified by

$$\boxed{\| W\Delta M \|_{\Delta Z} = \left\| W\left(NL^{-1}F(I + NL^{-1}F - F)^{-1} - F \right) \right\|_{\Delta Z}} \quad (31)$$

Lemma 5: Representation of ΔM as a Cascade of Operators. Under the assumptions of Definition 2, we have that

$$\Delta M = (I - F)(N - L)L^{-1}F\left(I + (N - L)L^{-1}F \right)^{-1}. \quad (32)$$

Proof. See Appendix F.

Lemma 6: Nonlinearity Measures in Definition 1 and Definition 2 are Equal for Stable N^{-1}, L^{-1}. When L^{-1} is stable, then the optimal choice $Q = L^{-1}F$ for Q in Lemma 4 yields

$$\Delta N = \Delta M. \quad (33)$$

Proof. Obvious, by substituting $Q = L^{-1}F$ into Eq. 26.

Remark 6: Importance of Lemma 6. The above Lemma 6 implies that when the plant and its model have stable inverses, the nonlinear closed loop with nonlinear plant and linear IMC (Figure 1) has the same distance from the following two ideal closed loops: (a) A linear IMC loop with linear plant and controller; and (b) a nonlinear IMC loop with nonlinear plant and controller. Note that these two closed loops are different.

Main result: How close to a linear closed loop can the nonlinear closed loop be designed?

Definition 1 requires that the operator $I + NQ - LQ$ be invertible and $(I + NQ - LQ)^{-1}$ be stable over corresponding sets. In addition, the direct effect of the Youla parameter Q on closed-loop nonlinearity should be easy to assess for controller synthesis. The following theorem resolves both of these issues.

Theorem 1: Upper and Lower Bounds on Control-Relevant Nonlinearity of a Stabilized Closed-Loop. Let the operators N, L, Q, and W represent a nonlinear plant, linear model, linear Youla parameter (Figure 1), and linear low-pass filter, respectively. Consider a set E and let the set Z be defined as

$$\boxed{Z \triangleq (I + NQ - LQ)(E)} \quad (34)$$

Let

$$\boxed{\gamma \triangleq \| (N - L)Q \|_{\Delta E} < 1} \quad (35)$$

Then:

(1). The operator $I + NQ - LQ$ is invertible over the set Z.

(2). The operator $(I + NQ - LQ)^{-1}$ is stable over the set Z.

(3) The control-relevant nonlinearity of the closed loop is bounded as

$$\boxed{\upsilon_{\min} \triangleq \frac{\|W(I-LQ)(N-L)Q\|_{\Delta E}}{\|I+(N-L)Q\|_{\Delta E}} \le \|W\Delta N\|_{\Delta Z} \le \frac{\|W(I-LQ)(N-L)Q\|_{\Delta E}}{1-\|(N-L)Q\|_{\Delta E}} \triangleq \upsilon_{\max}} \tag{36}$$

Proof. See Appendix G.

Corollary 2: Weaker Variant of Theorem 1. Under the assumptions of Theorem 1 we have

$$\boxed{\eta_{\min} \triangleq \frac{\|W(I-LQ)(N-L)Q\|_{\Delta E}}{1+\|(N-L)Q\|_{\Delta E}} \le \|W\Delta N\|_{\Delta Z} \le \|W(I-LQ)\| \frac{\|(N-L)Q\|_{\Delta E}}{1-\|(N-L)Q\|_{\Delta E}} \triangleq \eta_{\max}} \tag{37}$$

Proof. See Appendix H.

Remark 7: Significance of Theorem 1. (1) In addition to establishing lower and upper bounds of the control-relevant closed-loop nonlinearity quantifier of Definition 1, Theorem 1 also provides a sufficient condition (Eq. 35) for robust stability (over corresponding input sets) of a nonlinear closed-loop involving a nonlinear plant and a linear controller. In fact, the closed loop may turn from stable to unstable when external inputs increase beyond a certain point, thus violating Eq. 35 as subsequent simulation examples in the next section will clearly demonstrate. Equation 35 is certainly a sufficient condition. However, the examples in the next section will indicate that it is not necessarily conservative.

(2) Equations 36 and 37 make it clear that, for a given low-pass filter W, the nonlinearity of the closed loop depends on

(a) the nonlinearity of the controlled plant (difference between N and L);

(b) the linear model L;

(c) the linear controller Q; and

(d) the set E and, consequently, Z.

It is obvious that, when the plant is linear, that is, $N = L$, then the nonlinearity of the closed loop is trivially equal to zero.

When the plant is nonlinear, that is, $N \neq L$, it is clear that different choices of Q, that is, different controllers, will result in closed-loop nonlinearities with different bounds in Eqs. 36 and 37. The upper bound in Eq. 37 provides additional insight: It is the product of two terms, namely

$$\boxed{\alpha \triangleq \|W(I-LQ)\|} \tag{38}$$

and

$$\boxed{\beta \triangleq \frac{\|(N-L)Q\|_{\Delta E}}{1-\|(N-L)Q\|_{\Delta E}} \triangleq \frac{\gamma}{1-\gamma}} \tag{39}$$

For a given low-pass filter W, the first term $\|W(I-LQ)\|$ is the norm of the weighted sensitivity function of the ideal *linear* closed loop. It depends only on L and Q, that is, on the linear feedback controller designed for the nonlinear process. It is evident that *linear controller design that employs a linear process model L and selects Q by making* $\|W(I-LQ)\|$ *small will also tend to make the nonlinearity of the closed-loop small.*

The second term

$$\frac{\|(N-L)Q\|_{\Delta E}}{1-\|(N-L)Q\|_{\Delta E}}$$

depends on both the feedback controller and the open-loop nonlinearity $N-L$ of the process. This term provides a *direct link between open-loop nonlinearity and linear controller design*. It should also be stressed that if a "small" upper bound $\upsilon_{\max}$ can be established, then it clearly indicates that the closed loop is "fairly" linear, even if the value of that upper bound is orders of magnitude apart from an (obviously even smaller) lower bound $\upsilon_{\min}$. Conversely, if a "large" value of the lower bound $\upsilon_{\min}$ can be established, then it clearly indicates that the closed loop is "fairly" nonlinear, regardless of the value of the upper bound $\upsilon_{\max}$. In fact, controller design aiming at establishing a small value for the upper bound accomplishes the task of generating a fairly linear closed loop, regardless of the lower bound.

(3) Let us further elaborate on the previous Remark 7-2: Assume, as before, that W is a low-pass filter, and that L, in addition to being stable, also has a stable inverse. Then, the standard IMC design for Q is $Q = L^{-1}F$ where the filter F typically corresponds to a transfer function

$$G_F(s) = \frac{1}{(\lambda s+1)^r} \tag{40}$$

although more sophisticated filters may be considered. If the choice of Q were not required to satisfy the inequality (Eq. 35), then the term $\|W(I-LQ)\|$ in the righthand side of Eq. 37 could be made arbitrarily small by making the time constant λ of the filter G_F in Eq. 40 arbitrarily small, because

$$\lim_{\lambda\to 0}\|W(I-LQ)\| = \lim_{\lambda\to 0}\|W(I-F)\| = \lim_{\lambda\to 0}\sup_{\omega}\left|W(j\omega)\frac{(\lambda j\omega+1)^r-1}{(\lambda j\omega+1)^r}\right| = 0. \tag{41}$$

This would make closed-loop nonlinearity arbitrarily small. However, the presence of inequality (Eq. 35) poses constraints on how small λ can be made, and, consequently, closed-loop nonlinearity may not be made arbitrarily small. The effect of Q on closed-loop nonlinearity will be made clear

after the computation of incremental norms over sets has been discussed in the next section.

Note also that if L^{-1} is not stable, then $\|W(I-LQ)\|$ cannot be made arbitrarily small, even if Q is not required to satisfy the inequality (Eq. 35). This limitation of systems with unstable inverses is in addition to well-known bandwidth and inverse-response limitations of such systems (Skogestad and Postlethwaite, 1996).

(4) It is instructional to continue the analysis of the above Remark 7-2 under the additional assumptions that N^{-1} and L^{-1} are stable. In that case, Lemma 5 and Lemma 6 imply that closed-loop nonlinearity, defined through either Definition 1 or Definition 2, is bounded as

$$\|W\Delta N\|_{\Delta Z} = \|W\Delta M\|_{\Delta Z} \le \|W(I-F)\| \frac{\|N-L\|_{\Delta L^{-1}F(E)}\|L^{-1}F\|}{1-\|N-L\|_{\Delta L^{-1}F(E)}\|L^{-1}F\|}. \quad (42)$$

If induced 2-norms and incremental norms are used in the above Eq. 42, then Eq. 42 implies that there always exists a filter F as in Eq. 40 that makes

$$\boxed{\|W\Delta N\|_{\Delta Z} = \|W\Delta M\|_{\Delta Z} \le \frac{\dfrac{\|N-L\|_{\Delta L^{-1}F(E)}}{|G_L(0)|}}{1-\dfrac{\|N-L\|_{\Delta L^{-1}F(E)}}{|G_L(0)|}}} \quad (43)$$

as long as

$$\boxed{\frac{\|N-L\|_{\Delta L^{-1}F(E)}}{|G_L(0)|} < 1} \quad (44)$$

The great importance of Eq. 43 subject to Eq. 44 is that it provides a direct link between open-loop and closed-loop nonlinearity. In particular, it indicates that if "open-loop" nonlinearity is "small," that is,

$$\frac{\|N-L\|_{\Delta L^{-1}F(E)}}{|G_L(0)|} < \xi \ll 1$$

then closed-loop nonlinearity is also going to be small, that is, $\|W\Delta N\|_{\Delta Z} \le \xi/(1-\xi) \approx \xi$. Note that the magnitude of the open-loop nonlinearity is to be computed over the set $L^{-1}F(E)$, which is partly determined by the IMC filter F. However, the steady-state gain of F is 1, and, consequently, the choice of F is going to be irrelevant if the approximation scheme of Corollary 3 below is used for the computation of $\|N-L\|_{\Delta L^{-1}F(E)}$.

(5) The low-pass filter W, acting on ΔN, can be thought of as a filter acting on the difference between the outputs of the nonlinear closed loop and the ideal linear closed loop. Using W, one can do a form of *frequency analysis and design for the nonlinear closed loop*, as follows: Assume that an upper bound on the frequency content Ω of the set point changes or output disturbances is roughly known. Select a filter W that has amplitude ratio approximately 1 for frequencies in Ω and approximately zero for higher frequencies. Then, a linear controller can be designed that makes the (high-pass) sensitivity function $1-G_L(j\omega)G_Q(j\omega)$ of the ideal linear closed loop "almost 0" (and the (low-pass) complementary sensitivity function $G_L(j\omega)G_Q(j\omega)$ of the ideal linear closed loop "almost 1") over frequencies in Ω. This results in $\|W(I-LQ)\| \approx 0 \Rightarrow \|W\Delta N\| \approx 0$, by Eq. 37. Therefore, there can be a guarantee that the outputs of the nonlinear loop and of the ideal linear loop will be almost identical over Ω. This is illustrated in Example 7. Note that the preceding result does not guarantee anything about the behavior of the nonlinear closed-loop output in the frequency range outside Ω. In fact, intermodulation distortion is a well known phenomenon in which frequencies not included in the input may appear in a system's output. On the other hand, passivity results in the frequency domain may be established. Therefore, the implications of the preceding discussion need to be further investigated.

(6) A direct counterpart of Eq. 35 is well known in linear robust control theory (for example, Morari and Zafiriou, 1989, pp. 33, 66) in the form of the inequality

$$\sup_{\omega,\tilde{\mathrm{P}}} \left[(\mathrm{P}(j\omega)-\tilde{\mathrm{P}}(j\omega))\mathrm{Q}(j\omega)\right] < 1, \quad (45)$$

which is necessary and sufficient for robust closed-loop stabilization of the stable linear plant $\mathrm{P}(s)$ by a linear IMC controller with linear model $\tilde{\mathrm{P}}(s)$. The magnitude of external inputs is not an issue for the linear case.

(7) Theorem 1 is a form of a small-gain theorem, the small-gain condition being Eq. 35. It is interesting to contrast Theorem 1 to well known small-gain Theorems for standard (as opposed to model-based) nonlinear feedback loops with nonlinear operators N and C for the plant and classical feedback controller, respectively. The standard Small-Gain Theorem asserts that the closed loop is finite-gain stable, if the induced norm $\|NC\|_i < 1$ (Desoer and Vidyasagar, 1975, p. 41). The condition $\|NC\|_i < 1$ is prohibitively conservative for practical use. To support that claim, one need only consider the induced 2-norm

$$\|PC\|_{i2} \triangleq \sup_{x \ne 0} \frac{\|PCx\|_2}{\|x\|_2},$$

with P and C being single-input-single-output (SISO) linear operators, corresponding to the transfer functions $G_P(s)$ and $G_C(s)$ in the Laplace domain. In that case, $\|PC\|_{i2} = \sup_{\omega} |G_P(j\omega)G_C(j\omega)|$, and the standard Small-Gain Theorem implies that closed-loop stability would be guaranteed if

$$\sup_{\omega} |G_P(j\omega)G_C(j\omega)| < 1. \quad (46)$$

This inequality, however, may be violated by important classes of stabilizing controllers, such as controllers with integral action (such as PID controllers), for which $\sup_{\omega}|G_P(j\omega)G_C(j\omega)| = \infty$. In fact, it is well known that a nonconservative form of Eq. 46 is the familiar Nyquist stability criterion $|G_P(j\omega_{co})G_C(j\omega_{co})| < 1$, where ω_{co} is the crossover frequency. On the other hand, Eq. 35 in Theorem 1 *does* encompass PID controllers (Morari and Zafiriou, 1989, p. 67).

(8) Theorem 1 makes explicit use of the sets E (which contains the signal ϵ in Figure 1, for example,

$$E = \left\{ \epsilon \,|\, \| \epsilon \|_p \le \epsilon_{\max} \right\}) \tag{47}$$

$(1 \le p \le \infty)$ and $Z \triangleq \{z | z = (I + NQ - LQ)\epsilon\}$ (which contains either set points or disturbances, Eq 34). Knowledge of the set E combined with Eq. 35 can be used to explicitly characterize a superset of the set Z as

$$Z \subseteq \Xi \triangleq \left\{ z \,|\, \| z \| \le \left(1 + \| (N-L)Q \|_{\Delta E}\right) \epsilon_{\max} \le 2\epsilon_{\max} \right\}. \tag{48}$$

The meaning of the above inequality Eq. 48 is that Theorem 1 cannot be guaranteed to be valid for set points or disturbances with norms larger than $(1 + \| (N-L)Q \|_{\Delta E})\epsilon_{\max} \le 2\epsilon_{\max}$. While Eq. 48 does not provide an exact characterization of the set Z, we demonstrate through a number of examples in the sequel that Eq. 48 is not necessarily conservative. In fact, we have found that it is frequently very accurate.

(9) Note that Theorem 1 is also true under the weaker assumption that the composition LQ of the operators L and Q is linear, rather than each of L and Q being linear. This result could be used in robust nonlinear controller design. For example, if a nonlinear plant model $\tilde{N}$ is used in place of L, with $\tilde{N}^{-1}$ stable, then the standard nonlinear controller design $Q = \tilde{N}^{-1}F \Leftrightarrow \tilde{N}Q = F$ with a linear filter F can be used, and Theorem 1 can be used to design F for robust stability and performance. In that case, Eq. 36 places bounds on the distance between the nominal and the actual closed-loop operators.

Insight provided by and computation of incremental norms over sets

The bounds placed on closed-loop nonlinearity by Theorem 1 or Corollary 2 through Eqs. 36 and 37 are functions of the incremental norms $\| W(I - LQ)(N - L)Q \|_{\Delta E}$, $\| I + (N-L)Q \|_{\Delta E}$, and $\| (N-L)Q \|_{\Delta E}$. In addition, these bounds rely on satisfaction of the inequality $\| (N-L)Q \|_{\Delta E} < 1$ in Eq. 35. Therefore, to use Theorem 1 or Corollary 2 for controller analysis and, more importantly, design, it is clear that one must be able to:

(a) Reliably compute the incremental norms $\| W(I - LQ)(N - L)Q \|_{\Delta E}$, $\| I + (N-L)Q \|_{\Delta E}$, and $\| (N-L)Q \|_{\Delta E}$ for a given filter W, nonlinear plant N, linear model L, and controller Q (analysis).

(b) Assess the effect of the controller Q on $\| W(I - LQ)(N - L)Q \|_{\Delta E}$, $\| I + (N-L)Q \|_{\Delta E}$, and $\| (N-L)Q \|_{\Delta E}$ for a given filter W, nonlinear plant N, and linear model L, in order to synthesize a controller Q (synthesis).

The following theorem is crucial for both of the above tasks:

Theorem 2: Computation of Incremental Norms Over Sets. Let $M: V \to X$ be an unbiased nonlinear operator, and let $L_{u_0}: V \to X$ be its linearization approximation around the trajectory u_0 (Willems, 1971), where the sets V and X are subsets of Banach spaces (such as L_{pe}, $p \in [1, \infty]$), and V is convex. Then

$$\| M \|_{\Delta V} = \sup_{\substack{u_1, u_2 \in V \\ u_1 \ne u_2}} \frac{\| Mu_1 - Mu_2 \|}{\| u_1 - u_2 \|} = \sup_{u_0 \in V} \| L_{u_0} \| \tag{49}$$

Proof. See Nikolaou and Manousiouthakis (1989).

The above Theorem 2 indicates that, for the computation of $\| M \|_{\Delta V}$, direct optimization that determines

$$\sup_{\substack{u_1, u_2 \in V \\ u_1 \ne u_2}} \frac{\| Mu_1 - Mu_2 \|}{\| u_1 - u_2 \|}$$

can be replaced by much simpler optimization that finds $\sup_{u_0 \in V} \| L_{u_0} \|$, because the operator L_{u_0} is linear time-varying, hence, explicit expressions exist for $\| L_{u_0} \|$ for many norm functions (such as p-norms, $p = 1, 2, \infty$). Indeed, Nikolaou and Manousiouthakis (1989) have demonstrated that finding $\sup_{u_0 \in V} \| L_{u_0} \|$ is feasible via nonsmooth optimal control, albeit cumbersome. The following heuristic approximation of Eq. 49, within the spirit of the above tasks a and b, allows the computation of $\| M \|_{\Delta V}$ via trivial computations.

Corollary 3: Approximate Computation of Incremental Norms Over Sets. Under the conditions of Theorem 2

$$\| M \|_{\Delta V} \approx \sup_{\substack{u_0 \in V \\ u_0 \text{ constant}}} \| L'_{u_0} \| \tag{50}$$

where the operator L'_{u_0} appearing in the righthand side of the above Eq. 50 is the linearization of M around steady states (constant) u_0 in the set V.

Remark 8: Importance of Corollary 3. (1) Because the operator L'_{u_0} is linear time-invariant, well known explicit formulas exist for $\| L'_{u_0} \|$ for many norm functions (such as p-norms, $p = 1,2,\infty$). Therefore, $\sup_{\substack{u_0 \in V \\ u_0 \text{ constant}}} \| L'_{u_0} \|$ can be searched for efficiently.

(2) Theorem 1 relies on the inequality (Eq. 35), which involves $\| (N-L)Q \|_{\Delta E}$. According to Theorem 2, to compute $\| (N-L)Q \|_{\Delta E}$, one needs to linearize $(N-L)Q$ around trajectories ϵ_i belonging to the set E (see Figure 1 and Remark 7-8) and compute the supremum over all ϵ_i that play the role of u_0 in the righthand-side of Eq 49. Corollary 3 requires only constant values of ϵ_i for the approximate computation of $\| (N-L)Q \|_{\Delta E}$ according to Eq. 50. Computation can proceed as follows:

(a) Consider a steady-state (constant) value ϵ_i in the set $E = \{\epsilon \,|\, \| \epsilon \| \le \epsilon_{\max}\}$.

(b) Find the corresponding steady-state value u_i of $Q\epsilon_i$. That value is well defined, because Q is designed to be a globally stable linear time-invariant operator.

(c) Find L_{u_i}, the linearization of the nonlinear operator N around the steady-state u_i of Part b.

(d) Consider the operator $(L_{u_i} - L)Q$ in place of the linearization of $(N-L)Q$ around ϵ_i.

(e) Compute $\| (L_{u_i} - L)Q \|$, where the norm function denotes the induced norm of the operator $(L_{u_i} - L)Q$ corre-

sponding to the norm $\|(N-L)Q\|_{\Delta E}$. For example, one can use the induced 2-norm [H-infinity norm of the corresponding transfer function $G_{(L_{u_i}-L)Q}(j\omega)$] that is

$$\left\|\left(L_{u_i}-L\right)Q\right\|_{i2}=\sup_{\omega}\left|\left(G_{L_{u_i}}(j\omega)-G_L(j\omega)\right)G_Q(j\omega)\right| \quad (51)$$

or the induced ∞-norm, that is

$$\left\|\left(L_{u_i}-L\right)Q\right\|_{i\infty}=\|h\|_1=\int_0^{\infty}|h(t)|dt<\infty \quad (52)$$

where $h(t)$ is the impulse response of $(L_{u_i}-L)Q$ (Desoer and Vidyasagar, 1975).

(f) Repeat the above steps a through e for increasing values of ϵ_i.

(3) The above procedure for computation of incremental norms can obviously be applied to the computation of $\|W(I-LQ)(N-L)Q\|_{\Delta E}$ and $\|I+(N-L)Q\|_{\Delta E}$ that appear in Eq. 36 .

(4) Whether the induced 2-norm (Eq. 51), induced ∞-norm (Eq. 52), or any other induced norm that is easy to compute through Eq. 50 should be used in Theorem 1 depends on the closed-loop performance criterion. For example, if the root-mean-square (RMS) error is important, the 2-norm should be used. If maximum errors are important, then the ∞-norm should be used. This will be demonstrated in the Examples section.

(5) Of particular importance is the use of the 2-norm with Theorem 1 and Corollary 3 in synthesizing a stabilizing controller Q. Let $Q=L_{\text{inv}}F$ be a candidate controller where L_{inv} is a stable approximation of L^{-1} (Morari and Zafiriou, 1989, Chapter 4). Combining Eq. 35 with Eqs. 50 and 51 we get that Q is stabilizing over the set E if

$$\sup_{\omega}\left|\left(G_{L_{u_i}}(j\omega)-G_L(j\omega)\right)G_{L_{\text{inv}}}(j\omega)G_F(j\omega)\right|<1 \quad (53)$$

for all u_i defined in Remark 8-2b. Thus, one can design a linear feedback controller that stabilizes the nonlinear closed loop by designing a linear Q through selection of a time constant λ for the filter $G_F(s)=1/(\lambda s+1)^r$ such that Eq. 53 is satisfied. A Bode plot can provide a particularly simple and intuitive graphical aid for the selection of λ through satisfaction of Eq. 53, by rewriting Eq. 53 as

$$\left|\left(G_{L_{u_i}}(j\omega)-G_L(j\omega)\right)G_{L_{inv}}(j\omega)\right|<\frac{1}{|G_F(j\omega)|}=\frac{1}{(\lambda^2\omega^2+1)^{r/2}}\ \text{for all}\ \omega \quad (54)$$

for all u_i defined in Remark 8-2b, and requiring that the Bode plot of the righthand side of Eq. 54 does not intersect the family of Bode plots of the lefthand side. This will be shown in the next section.

(6) When the operator M in Eq. 50 is one of the operators $(N-L)Q$, $W(I-LQ)(N-L)Q$ or $I+(N-L)Q$, which appear in Theorem 1, then the operator N (plant) must be linearized around several steady states. This can be done either by linearizing a first-principles nonlinear model of the controlled plant around desired steady states, or by developing multiple linear models from experimental data, each model being valid around a steady state of interest. Given that the development of multiple linear models around various steady states is not uncommon in industry, *Corollary 3 substantially enhances that practice by indicating how to use such models for rigorous and computationally efficient analysis and synthesis of model-based controllers for nonlinear processes.*

(7) Note that obviously $\|M\|_{\Delta V}\geq\sup_{\substack{u_0\in V\\ u_0\ \text{constant}}}\|L'_{u_0}\|$. An upper bound to $\|M\|_{\Delta V}$ would be preferable for Eqs. 35, 36, or 37. However, we are not aware of such a bound.

Recapitulating: linear controller design for nonlinear systems — when and how

The preceding results can be organized in a well defined, computationally effective methodology of linear controller design for open-loop stable nonlinear systems, as follows:

(1) Obtain linear time-invariant dynamic process models around steady states of interest, for disturbances and set points corresponding to the sets E and Z, as indicated by Eqs. 47 and 48 in Remark 7-8. Such models may be obtained either by direct experimentation or by linearization of an available nonlinear dynamic process model.

(2) Use a linear process model L in a linear IMC controller parametrized in terms of the time-constant λ in the filter F (Eq. 40) of the Youla parameter Q (Figure 1).

(3) Apply Corollary 3 (Remark 8-2) to select the smallest value $\lambda_{\min}$ of λ that satisfies the closed-loop stability condition, the inequality (Eq. 35) of Theorem 1, as discussed in Eqs. 51 or 52.

(4) Apply Corollary 3 to compute incremental norms and subsequently compute closed-loop nonlinearity bounds that appear in Eq. 36 of Theorem 1 or Eq. 37 of Corollary 2, for various values of the IMC filter time-constant λ greater than the value $\lambda_{\min}$ computed in the above part 3.

Examples

In all examples that follow, single-input-single-output nonlinear models, as in Eq. 4, are available. The variables u and y refer to each model's input and output in deviation form. Corollary 3 is used for the computation of all incremental norms. Unless otherwise specified, $p=2$ in all norms and incremental norms, and the low-pass weighting factor W is identity.

Example 1: Closed-Loop Stability and Instability Over Different Operating Ranges. Henson and Seborg (1990) studied the control of a system composed of two CSTRs in series. The irreversible exothermic reaction $A\rightarrow B$ occurs in the two reactors. The system is modeled by the nonlinear differential equations

$$\frac{dC_{A1}}{dt}=\frac{q}{V_1}\left(C_{Af}-C_{A1}\right)-k_0C_{A1}\exp\left(-\frac{E}{RT_1}\right) \quad (55)$$

Table 1. Parameters of 2-CSTR System in Example 1 (Henson and Seborg, 1990)

Variable	Definition	Value
C_{A1}, C_{A2}	Conc. of species A in CSTRs 1 and 2	State variables
T_1, T_2	Temp. of CSTRs 1 and 2	State variables
q_c	Coolant flow rate	Input variable
C_{A2}	See above	Output variable
C_{Af}	Feed conc. of species A	1 mol/L
T_f	Feed temp.	350 K
T_{cf}	Coolant feed temp.	350 K
q	Feed flow rate	100 L/min
E/R	Activation energy	1×10^4 K
$V_1 = V_2$	Volumes of CSTRs 1 and 2	100 L
k_0	Reaction rate constant	7.2×10^{10} min^{-1}
$-\Delta H$	Heat of reaction	4.78×10^{10} J/mol
$hA_1 = hA_2$	(heat-transfer coefficient)$\times$ (area)	1.67×10^5 J/min/K
$C_p = C_{pc}$	Specific heat	0.239 J/g/K
$\rho = \rho_c$	Density	1000 g/L
q_{cs}	Steady-state coolant flow rate	100 L/min
C_{A1s}	Steady-state conc. of A in CSTR 1	0.088228 mol/L
C_{A2s}	Steady-state conc. of A in CSTR 2	0.0052926 mol/L
T_{1s}	Steady-state temp. of CSTR 1	441.2193 K
T_{2s}	Steady-state temp. of CSTR 2	449.4746 K

$$\frac{dT_1}{dt} = \frac{q}{V_1}(T_f - T_1) + \frac{(-\Delta H)k_0 C_{A1}}{\rho C_p}\exp\left(-\frac{E}{RT_1}\right) + \frac{\rho_c C_{pc}}{\rho C_p V_1} q_c \left(1 - \exp\left(-\frac{hA_1}{q_c \rho_c C_{pc}}\right)\right)(T_{cf} - T_1) \quad (56)$$

$$\frac{dC_{A2}}{dt} = \frac{q}{V_2}(C_{A1} - C_{A2}) - k_0 C_{A2}\exp\left(-\frac{E}{RT_2}\right) \quad (57)$$

$$\frac{dT_2}{dt} = \frac{q}{V_2}(T_1 - T_2) + \frac{(-\Delta H)k_0 C_{A2}}{\rho C_p}\exp\left(-\frac{E}{RT_2}\right) + \frac{\rho_c C_{pc}}{\rho C_p V_2} q_c \left(1 - \exp\left(-\frac{hA_2}{q_c \rho_c C_{pc}}\right)\right) \times \left(T_1 - T_2 + \exp\left(-\frac{hA_1}{q_c \rho_c C_{pc}}\right)(T_{cf} - T_1)\right). \quad (58)$$

The concentration of the reactant at the exit of the second CSTR C_{A2} is the controlled variable, and the coolant flow rate q_c (common for both reactors) is the manipulated variable. Notation and parameter values are provided in Table 1.

Steady-state operation around the high-conversion of the three possible steady states of this system is considered. Linearization of the nonlinear model around that steady state yields the linear model L (for deviation input and output variables) with

$$G_L(s) = \frac{0.0003664s^2 + 0.0513s + 0.1391}{s^4 + 21.85s^3 + 116.8s^2 + 366.8s + 432.9} \quad (59)$$

This model is used for the design of an IMC controller as in Figure 1, with $Q = L^{-1}F$ where

$$G_F(s) = \frac{1}{(\lambda s + 1)^2}. \quad (60)$$

Table 2 shows bounds of closed-loop nonlinearity according to Theorem 1 (Eq. 36) for the upper bound and Eq. 37 for the lower bound), as well as values of $\gamma \triangleq \|(N - L)Q\|_{\Delta E}$ in Eq. 35, for different values of λ in Eq. 60. Rows of Table 2 correspond to increasing steady-state values of ϵ, (Eq. 47), that is, increasing operating ranges of the system, as discussed in Remark 7 and Remark 8. Steady-state values of the

Table 2. Lower and Upper Bounds of Closed-Loop Nonlinearity in Example 1 According to Theorem 1 and Corollary 3, for different values of λ in Eq. (60), $p = 2$

			$\lambda = 0.1$			$\lambda = 1$			$\lambda = 5$ or 10		
ϵ_s	y_s	u_s	$\eta_{\min}$	$\upsilon_{\max}$	γ_2	$\eta_{\min}$	$\upsilon_{\max}$	γ_2	$\eta_{\min}$	$\upsilon_{\max}$	γ_2
0	0	0	0	0	0	0	0	0	0	0	0
—	—	—	—	—	—	—	—	—	—	—	—
1.25×10^{-3}	1.4×10^{-3}	3.8896	0.2460	1.4485	0.7096	0.1693	0.3091	0.2923	0.153	0.2809	0.2923
1.50×10^{-3}	1.8×10^{-3}	4.6676	0.2840	12.0216	0.9538	0.2006	0.4297	0.3635	0.181	0.3885	0.3635
1.75×10^{-3}	2.1×10^{-3}	5.4455	NA	NA	**1.2625**	0.2312	0.5951	0.4404	0.208	0.5353	0.4404
—	—	—	—	—	—	—	—	—	—	—	—
2.50×10^{-3}	3.3×10^{-3}	7.7793				0.3206	1.9065	0.5488	0.2831	1.6836	0.4847
2.75×10^{-3}	3.7×10^{-3}	8.5572				0.3499	3.5377	0.82	0.3067	3.1014	0.82
3.00×10^{-3}	4.2×10^{-3}	9.3351				0.4582	14.558	0.939	0.3297	10.4762	0.939
3.25×10^{-3}	4.7×10^{-3}	10.113				NA	NA	**1.3422**	NA	NA	**1.0710**

process output y_s and input u_s corresponding to ϵ_s (that is, $u_s = (Q\epsilon)_s$ and $y_s = (NQ\epsilon)_s$) are also shown to provide direct estimates of operating ranges over which results are valid.

According to Table 2, when $\lambda = 1$, Theorem 1 guarantees closed-loop stability for set point pulses of amplitude $+4.2\times 10^{-3}$ (y_s column), because the corresponding $\gamma = 0.939 < 1$. This prediction is verified in Figure 4, which shows closed-loop responses of (a) the nonlinear process Eqs. 55–58 with the designed IMC controller ($\lambda = 1$), and (b) the linearized system (Eq. 59), with the same IMC controller (perfect model assumption) for pulse set point change of amplitude $+4.2\times 10^{-3}$ mol/L.

Theorem 1 does not guarantee closed-loop stability for set point pulses of amplitude 4.7×10^{-3} or larger (y_s column), because the corresponding $\gamma = 1.3422 > 1$. This prediction is verified in Figure 5, which shows responses of the same two closed-loop systems as in Figure 4, for pulse set point change of amplitude $+5.2\times 10^{-3}$ mol/L.

Example 2: Linear Feedback May Create a Closed Loop Less Nonlinear than the Open Loop. In addition to predicting operating regions of closed-loop stability or instability, Table 2 of Example 1 can also be used to predict how closed-loop and open-loop nonlinearities compare with each other. For such a comparison to be meaningful, open-loop and closed-loop nonlinearities must first be appropriately scaled, because open-loop nonlinearity refers to the mapping $N{:}u \to y$, while closed-loop nonlinearity refers to the mapping $N_{ry}{:}r \to y$ (Eq. 21 and Figure 1). Therefore, for each nonlinear operator, we scale its incremental norm (nonlinearity quantifier) by dividing it by the norm of a corresponding ideal linear operator, as shown next. Closed-loop nonlinearity is scaled as

$$\frac{\|W\Delta N\|_{\Delta Z}}{\|W(I-LQ)\|} \hat{=} \frac{\left\|W\left(NQ(I+NQ-LQ)^{-1}-LQ\right)\right\|_{\Delta Z}}{\|W(I-LQ)\|} \tag{61}$$

according to Eq. 25 in Definition 1. Because, for this example, $W = I$, $LQ = F$, and 2-norms are used throughout, we have that $\|W(I-LQ)\| = 1$; hence, the values of $\eta_{\min}$ and $\upsilon_{\max}$ of Table 2 will not be altered as a result of scaling. Open-loop nonlinearity is scaled as

$$\frac{\|N-L\|_{\Delta Q(E)}}{\|L\|} \tag{62}$$

By Theorem 2 $\|N-L\|_{\Delta Q(E)} = \sup_{u_0 \in Q(E)} \|L_{u_0} - L\|$, hence

$$\frac{\|N-L\|_{\Delta Q(E)}}{\|L\|} \geq \frac{\|L_{u_0}-L\|}{\|L\|} \tag{63}$$

for a specific $u_0 \in Q(E) = L^{-1}F(E)$.

Let us consider as u_0 the steady-state input value $u_s = 7.7793$ that results in steady-state output value $y_s = +3.3\times 10^{-3}$. Straightforward linearization of N around this steady state yields

$$G'_{L_{u_0}}(s) = \frac{0.0006s^2 + 0.0495s + 0.1245}{s^4 + 15.98s^3 + 53.48s^2 + 154.4s + 226.3} \tag{64}$$

Application to Eq. 63 yields that the open-loop nonlinearity has a lower bound as

$$\frac{\|N-L\|_{\Delta Q(E)}}{\|L\|} \gtrsim 2.8. \tag{65}$$

On the other hand, Table 2 shows that, for $y_s = 3.3\times 10^{-3}$, the closed-loop nonlinearity has an upper bound as $\upsilon_{\max} = 1.906$ for $\lambda = 1$. Therefore

$$\frac{\|N-L\|_{\Delta Q(E)}}{\|L\|} > \frac{\|W\Delta N\|_{\Delta Z}}{\|W(I-LQ)\|} \tag{66}$$

indicating that *the closed loop is less nonlinear than the open loop*. This prediction is verified by comparing Figure 2, which shows evident open-loop nonlinearity, to Figure 4, which shows virtually no closed-loop nonlinearity for the even larger set point change $+4.2\times 10^{-3}$. It should be stressed that the above prediction involved extremely simple computations.

Example 3: Robustness of Linear Control for Nonlinear Process. The same system as in Example 1 is studied, with the addition of measurement delay of five time units to the system (Figure 1). The aim of this example is to apply inequality (Eq. 54) and associated graphical analysis for controller design, that is, selection of values of λ such that

$$\left|\frac{G_{L_{u_i}}(j\omega) - G_L(j\omega)}{G_L(j\omega)}\right| < \frac{1}{|G_F(j\omega)|} = \frac{1}{\lambda^2\omega^2 + 1} \text{ for all } \omega \tag{67}$$

for all u_i defined in Remark 8-2b. Figure 16 shows $1/|G_F(j\omega)|$ for various values of λ, and

$$\left|\frac{G_{L_{u_i}}(j\omega) - G_L(j\omega)}{G_L(j\omega)}\right|$$

for different u_i, both without delay in $G_{L_{u_i}}(j\omega)$ (solid lines) and with delay approximated by 5th-order Padé approximation (dashed lines). Recall that the linear model L does not include any measurement delay. When $\lambda = 10$ and $G_{L_{u_i}}(j\omega)$ includes the measurement delay, Figure 16 shows that the inequality (Eq. 67) is satisfied. Lower values of λ fail to satisfy Eq. 67. Therefore, IMC with $\lambda = 10$ guarantees robust stability of the closed loop in the presence of measurement delay.

This prediction is verified in Figure 8, which shows the response of the nonlinear closed loop with linear IMC and $\lambda = 10$ to a step change in the set point. The response of the ideal linear closed loop $I - F$ is also included in Figure 8. In contrast, Figure 7 shows the response of the nonlinear closed loop with linear IMC and $\lambda = 0.1$. It is clear that the process output fails to follow the set point.

Is this lack of robustness for $\lambda = 0.1$ due to the presence of measurement delay or to process nonlinearity? Figure 6 shows the response of a linear closed loop with a linear process L, measurement delay, and linear IMC employing a model L and filter F with $\lambda = 0.1$. The response is stable, as can be easily shown by computing the poles of the closed loop.

Table 3. Parameters of CSTR in Example 4

Variable	Definition	Value
C_A	Conc. of species A in CSTR	State variable
T	Temp. of CSTR	State and Output variable
F	Feed flow rate value	Input variable
C_{Ai}	Feed conc. of species A	8,008 mol/L
T_i	Feed temp.	373.3 K
T_c	Coolant feed temp.	532.6 K
E/R	Activation energy/Gas const.	8375 K
V	Volume of CSTR	1.36 m^3
k_0	Reaction rate const.	7.08×10^7 h^{-1}
$\frac{UA_t}{\rho C_p}$	$\frac{\text{(heat-transfer coeff.) } \times \text{ (transfer area)}}{\text{(density) } \times \text{ (specific heat)}}$	2.8 m^3/h
F_s	Steady-state feed flow rate	1.133 m^3/h
C_{As}	Steady-state conc. of A in CSTR	393.2 mol/m^3
T_s	Steady-state temp. of CSTR	547.6 K

Therefore, the poor response in Figure 7 is due to process nonlinearity.

Example 4: CSTR with Unstable Inverse. The irreversible exothermic reaction $A \rightarrow B$ occurs in a CSTR modeled as

$$\frac{dC_A}{dt} = \frac{F}{V}(C_{Ai} - C_A) - k_0 C_A \exp\left(-\frac{E}{RT}\right) \tag{68}$$

$$\frac{dT}{dt} = \frac{F}{V}(T_i - T) + Jk_0 C_A \exp\left(-\frac{E}{RT}\right) - \frac{UA_t}{\rho C_p V}(T - T_c) \tag{69}$$

The feed flow rate is the input and the CSTR temperature is the output. Notation and steady-state values are provided in Table 3. For these values, the CSTR has unstable inverse (unstable zero dynamics in nonlinear geometric control terminology). Note that the steady state of Table 3 is the high-conversion steady state of the three possible steady states of this CSTR. Linearization of Eqs. 68 and 69 around the steady state of Table 3 yields a linear model L with transfer function

$$G_L(s) = \frac{-128.2s + 332.3}{s^2 + 14.96s + 45.03} = \frac{-128.2(s - 2.5925)}{(s + 4.1775)(s + 10.7788)}. \tag{70}$$

Note the right-half-plane zero. This model is used for the design of an IMC controller in the form of $Q = L_{\text{inv}}F$ where

$$F = \frac{1}{(\lambda s + 1)^2} \tag{71}$$

and

$$L_{\text{inv}} = \frac{(s + 4.1775)(s + 10.7788)}{-128.2(-s - 2.5925)}. \tag{72}$$

Similarly to Table 2, Table 4 shows bounds of closed-loop nonlinearity according to Theorem 1 (Eq. 36 for the upper bound and Eq. 37 for the lower bound), as well as values of

Table 4. Lower and Upper Bounds of Closed-Loop Nonlinearity in Example 4 According to Theorem 1 and Corollary 3, for Different Values of λ in Eq. 71, $p = 2$

			$\lambda = 0.1$			$\lambda = 1$			$\lambda = 5$		
ϵ_s	y_s	u_s	$\eta_{\min}$	$\upsilon_{\max}$	γ_2	$\eta_{\min}$	$\upsilon_{\max}$	γ_2	$\eta_{\min}$	$\upsilon_{\max}$	γ_2
0	0	0	0	0	0	0	0	0	0	0	0
—	—	—	—	—	—	—	—	—	—	—	—
2.5	2.09	0.3387	—	—	—	0.1840	0.3216	0.2751	—	—	—
2.5	*2.09*	*0.3387*				*0.2561**	*0.4391**	*0.2631**			
11.25	5.39	1.5243	—	—	—	0.4117	9.149	0.9139	—	—	—
11.25	*5.39*	*1.5243*				*0.5535**	*9.2119**	*0.8866**			
—	—	—	—	—	—	—	—	—	—	—	—
11.75	5.426	1.5921	0.4828	16.65	0.9436	0.418	14.43	0.9436	0.3513	12.11	0.9436
12.00	5.438	1.6259	0.4868	22.92	0.9584	0.422	19.87	0.9584	0.3541	16.678	0.9584
12.25	5.446	1.6590	0.4908	36.049	0.9731	0.4253	31.24	0.9731	0.3568	26.211	0.9731
12.50	5.451	1.6937	0.4949	80.629	0.9878	0.4285	69.82	0.9878	0.3595	58.58	0.9878
12.75	5.452	1.7276	NA	NA	**1.0024**	NA	NA	**1.0024**	NA	NA	**1.0024**
13.00	5.450	1.7614			**1.0170**			**1.0170**			**1.0170**

*These numbers are computed for $p = \infty$.

$\gamma \hat{=} \|(N-L)Q\|_{\Delta E}$ in Eq. 35 for different values of λ in Eq. 71.

According to Table 4, the closed-loop stability condition $\gamma < 1$ (Eq. 35) is violated for $\epsilon_s \approx 12.75$ corresponding to a process output value of $y_s \approx 5.45$, and process input u_s approximately 150% of the original steady-state value F_s. Therefore, transition from stability to instability would be expected for set point changes around the above output value. Figure 10 verifies this prediction: For a set point step change of $+5.5$ (that is, temperature set point of 547.6 K), the output y initially attempts to reach that set point, but eventually escapes to a steady state of -174.3, that is, temperature of $547.6-174.3=373.3$ K, almost equal to the feed temperature. This new steady state is the low-conversion steady state of the three possible steady states of this CSTR. This example clearly shows that the proposed analysis clearly determined the point of departure from the linear response.

Table 4 also indicates that nonlinearity increases with increasing operating range, as expected. This is verified in Figure 17, which shows the scaled difference $(y_N - y_L/R)$ between the response of the nonlinear closed loop y_N and the ideal linear closed loop y_L to set point, changes R of magnitudes 2.09 (solid line) and 5.39 (dashed line). Both loops contain the same linear IMC controller with $\lambda = 1$. If the closed loop were linear, two lines should coincide.

Example 5: Van de Vusse CSTR. Chen et al. (1995) studied the nonlinearity of a CSTR in which the exothermic van de Vusse reactions $A \xrightarrow{k_1} B \xrightarrow{k_2} C$ and $A \xrightarrow{k_3} D$ take place. The CSTR is modeled by the following nonlinear equations

$$\frac{dC_A}{dt} = \frac{\dot{V}}{V_R}(C_{A0} - C_A) - k_1(T)C_A - k_3(T)C_A^2 \tag{73}$$

$$\frac{dC_B}{dt} = -\frac{\dot{V}}{V_R}C_B + k_1(T)C_A - k_2(T)C_B \tag{74}$$

$$\frac{dT}{dt} = \frac{\dot{V}}{V_R}(T_0 - T) - \frac{1}{\rho C_p}\left[k_1(T)C_A\Delta H_{RAB} + k_2(T)C_B\Delta H_{RBC} + k_3(T)C_A^2\Delta H_{RAD}\right] + \frac{k_w A_R}{\rho C_p V_R}(T_K - T) \tag{75}$$

$$\frac{dT_K}{dt} = \frac{1}{m_K C_{pK}}\left[\dot{Q}_K + k_w A_R(T - T_K)\right] \tag{76}$$

The flow rate $\dot{V}/V_R$ is the manipulated input and the concentration of the product B, C_B, is the controlled output. Parameter values used by Chen et al. (1995) are given in Table 5.

The optimal steady-state yield of this CSTR with respect to the product B is attained at the steady state shown in Table 5. However, as Chen et al. (1995) point out, the steady-state

Table 5. Van de Vusse CSTR Parameters for Example 5

Variable	Definition	Value
C_A, C_B	Conc. of species A and B	State variables
T, T_K	Temp. of CSTR and cooling jacket	State variables
C_B	Conc. of species A and B	Output variable
$\dot{V}/V_R$	Flow rate	Input variable
C_{A0}	Feed conc. of species A	5.1 mol/L
To	Feed temp.	104.9°C
Q_K	Heat removal rate steady-state value	-1113.5 kJ/h
k_{10}	Collision factor for reaction 1: $k_1(T) = k_{10}e^{-E_1/T}$	1.287×10^{12} h^{-1}
k_{20}	Collision factor for reaction 2: $k_2(T) = k_{20}e^{-E_2/T}$	1.287×10^{12}h^{-1}
k_{30}	Collision factor for reaction 3: $k_3(T) = k_{30}e^{-E_3/T}$	9.043×10^{9} (mol·A)$^{-1}$h^{-1}
E_1	Normalized activation energy for reaction 1	$-9{,}758.3$ K
E_2	Normalized activation energy for reaction 2	$-9{,}758.3$ K
E_3	Normalized activation energy for reaction 3	$-8{,}560$ K
ΔH_{RAB}	Enthalpies of reaction 1	4.2 kJ/molA
ΔH_{RBC}	Enthalpies of reaction 2	-11 kJ/molB
ΔH_{RAD}	Enthalpies of reaction 3	-41.85 kJ/molA
k_w	heat transfer coeff. for cooling jacket	4.032 kJ/(h·m^2·K)
A_R	Surface of cooling jacket	0.215 m^2
V_R	Reactor volume	0.01 m^3
m_K	Coolant mass	5.0 kg
C_{pK}	Heat capacity of coolant	2.00 kJ/(kg·K)
C_p	Heat capacity	3.01 kJ/(kg·K)
ρ	Density	0.9342 kg/L
C_{As}	Optimal steady-state conc. of A	2.1426 mol/L
C_{Bs}	Optimal steady-state conc. of B	1.0903 mol/L
T_s	Optimal steady-state temp. of CSTR	114.1466°C
T_{Ks}	Optimal steady-state temp. of cooling jacket	112.8479°C
$(\dot{V}/V_R)_s$	Optimal steady-state flow rate	0.2483 L/min
C_{As}	Suboptimal steady-state conc. of A	2.4837 mol/L
C_{Bs}	Suboptimal steady-state conc. of B	1.0725 mol/L
T_s	Suboptimal steady-state temp. of CSTR	114.0389°C
T_{Ks}	Suboptimal steady-state temp. of cooling jacket	112.7544°C
$(\dot{V}/V_R)_s$	Suboptimal steady-state flow rate	0.3316 L/min

Table 6. Lower and Upper Bounds of Closed-Loop Nonlinearity in Example 5 According to Theorem 1 and Corollary 3, for Different Values of λ in Eq. 78, $p = 2$

			$\lambda = 1$			$\lambda = 10$			$\lambda = 100$		
ϵ_s	y_s	u_s	$\eta_{\min}$	$\upsilon_{\max}$	$\times$	$\eta_{\min}$	$\upsilon_{\max}$	$\times$	$\eta_{\min}$	$\upsilon_{\max}$	$\times$
0	0	0	0	0	0	0	0	0	0	0	0
—	—	—	—	—	—	—					—
0.030	0.0178	0.0688	0.0552	1.0691	0.9018	0.207	4.009	0.9018	0.2366	4.583	0.9018
0.031	0.0178	0.0711	0.0565	1.892	0.942	0.211	7.007	0.942	0.2421	8.1057	0.942
0.032	0.0179	0.0734	0.0578	6.7322	0.983	0.216	25.23	0.983	0.2474	28.79	0.983
0.033	0.0179	0.0757	NA	NA	**1.0247**	NA	NA	**1.0247**	NA	NA	**1.0247**
0.034	0.0178	0.078	NA	NA	**1.0673**	NA	NA	**1.0673**	NA	NA	**1.0673**

gain changes sign at that operating point. Thus, linear controllers (with integral action) will not be able to stabilize this reactor. This fact is in agreement with Theorem 1. Indeed, Eq. 35 cannot possibly be satisfied, because there are always two infinitesimally differing inputs in the set E that can generate finite outputs of the operator $(N - L)Q$, making $\gamma = \infty$. Therefore, we will not study operation of this CSTR at the optimal operating point any further. Instead, we will study linear control of this nonlinear system at the suboptimal steady state shown in Table 5. The nonlinear system is linearized around this steady state. The linearized system L corresponds to the transfer function (for variables in deviation form)

$$G_L(s) = \frac{-1.073s^3 - 2.597s^2 - 0.8535s - 0.07328}{s^4 + 3.386s^3 + 3.417s^2 + 1.315s + 0.1682} \quad (77)$$

This model is used for the design of an IMC controller with $Q = L^{-1}F$ where

$$G_F(s) = \frac{1}{\lambda s + 1}. \quad (78)$$

Similarly to Table 2 and Table 4, Table 6 shows bounds of closed-loop nonlinearity according to Theorem 1 (Eq. 36 for the upper bound and Eq. 37 for the lower bound), as well as values of γ in Eq. 35, for different values of λ in Eq. 78. Figure 18 shows the values of γ when ϵ deviates from its steady-state value in the positive or negative direction. It can be observed that while γ exceeds 1, thus violating Eq. 35 when the magnitude of ϵ increases with $\epsilon > 0$ (in the direction where the optimal steady state can be reached), γ stays below 1 when the magnitude of ϵ increases with $\epsilon < 0$ (in the direction away from the optimal steady state). Thus, the van de Vusse CSTR is not severely nonlinear when steered away from the maximum conversion point. This conclusion is in agreement with a similar conclusion arrived at by Helbig et al. (2000).

It is also computationally straightforward to show that when γ exceeds 1, there is a bifurcation point, that is, the steady-state gain matrix becomes singular.

Example 6: Comparison of Closed-Loop Nonlinearities of Various Closed Loops. Comparison of Table 2, Table 4, and Table 6 reveals that the closed-loop nonlinearity bounds of the van de Vusse CSTR in Example 5 are an order of magnitude less than the closed-loop nonlinearity bounds in the reactors of Example 1 and Example 4. Therefore, one would expect lower closed-loop nonlinearity for the van de Vusse CSTR. This is indeed the case. Figure 10, Figure 12, and Figure 14 show the scaled difference $(y_N - y_L)/R$ between the response of the nonlinear closed loop y_N and the ideal linear closed loop y_L to set point changes R for each of the three systems. For each system, a pair of values of R were selected, corresponding to a pair of values for γ that were approximately the same for all three reactors. In this way, the stability margin for all three systems was kept approximately the same, while closed-loop nonlinearity was the main focus.

It is also interesting to observe the behavior of nonlinearity bounds as the value of the IMC filter coefficient λ increases, that is, the controller is tuned for faster closed-loop response. While the bounds for the van de Vusse CSTR (Ex-

Table 7. Lower and Upper Bounds of Closed-Loop Nonlinearity in Example 7 According to Theorem 1 and Corollary 3, for Different Values of λ in Eq. 78, $p = \infty$

			$\lambda = 1$			$\lambda = 5$			$\lambda = 10$		
ϵ_s	y_s	u_s	$\eta_{\min}$	$\upsilon_{\max}$	γ_∞	$\eta_{\min}$	$\upsilon_{\max}$	γ_∞	$\eta_{\min}$	$\upsilon_{\max}$	γ_∞
0	0	0	0	0	0	0	0	0	0	0	0
—	—	—	—	—	—	—	—	—	—	—	—
1.25×10^{-3}	1.4×10^{-3}	3.8896	0.2481	0.4502	0.2894	0.2145	0.3875	0.2874	0.214	0.386	0.2872
1.50×10^{-3}	1.8×10^{-3}	4.6676	0.2978	0.6331	0.3601	0.253	0.535	0.3575	0.252	0.533	0.3572
1.75×10^{-3}	2.1×10^{-3}	5.4455	0.3491	0.8898	0.4365	0.290	0.734	0.433	0.289	0.731	0.4328
—	—	—	—	—	—	—	—	—	—	—	—
2.75×10^{-3}	3.7×10^{-3}	8.5572	0.567	9.0822	0.8825	0.429	4.01	0.8066	0.428	3.981	0.8059
3.00×10^{-3}	4.2×10^{-3}	9.3351	NA	NA	**1.1503**	0.462	11.64	0.9237	0.460	11.48	0.923
3.25×10^{-3}	4.7×10^{-3}	10.113			**1.565**	NA	NA	**1.054**	NA	NA	**1.053**

Table 8. Lower and Upper Bounds of Closed-Loop Nonlinearity in Example 4 According to Theorem 1 and Corollary 3, for Different Values of λ in Eq. 71, $p=\infty$

			$\lambda=0.1$			$\lambda=1$			$\lambda=5$		
ϵ_s	y_s	u_s	$\eta_{\min}$	$\upsilon_{\max}$	γ_∞	$\eta_{\min}$	$\upsilon_{\max}$	γ_∞	$\eta_{\min}$	$\upsilon_{\max}$	γ_∞
0	0	0	0	0	0	0	0	0	0	0	0
—	—	—	—	—	—	—					—
11.75	5.4257	1.5921	0.592	20.361	0.9435	0.579	19.921	0.9435	0.487	16.658	0.9431
12.00	5.4377	1.6259	0.595	27.927	0.9583	0.584	27.405	0.9583	0.491	22.849	0.9579
12.25	5.446	1.659	0.598	43.687	0.973	0.588	43.005	0.973	0.495	35.64	0.9726
12.50	5.451	1.6937	0.601	96.772	0.9877	0.593	95.642	0.9877	0.499	77.677	0.9872
12.75	5.452	1.7276	NA	NA	**1.0023**	NA	NA	**1.0023**	NA	NA	**1.0018**

Table 9. Lower and Upper Bounds of Closed-Loop Nonlinearity in Example 5 According to Theorem 1 and Corollary 3, for Different Values of λ in Eq. 78, $p=\infty$

			$\lambda=1$			$\lambda=10$		
ϵ_s	y_s	u_s	$\eta_{\min}$	$\upsilon_{\max}$	γ_∞	$\eta_{\min}$	$\upsilon_{\max}$	γ_∞
0	0	0	0	0	0	0	0	0
—	—	—	—	—	—	—		
3.0×10^{-2}	0.0178	0.0688	0.088	1.8124	0.908	0.294	5.8338	0.904
3.1×10^{-2}	0.0178	0.0711	0.089	3.3445	0.948	0.3009	10.4878	0.944
3.2×10^{-2}	0.0179	0.0734	0.088	32.434	0.9946	0.3077	41.1243	0.9851
3.3×10^{-2}	0.0179	0.0757	NA	NA	**1.0363**	NA	NA	**1.0269**

ample 5) *increased* with increasing λ, nonlinearity bounds in Example 1 and Example 4 *decreased* with increasing λ, predicting corresponding trends in closed-loop nonlinearity. This prediction is verified in Figure 11, Figure 13, and Figure 15, which are the counterparts of Figure 18, Figure 12, and Figure 14, respectively, with higher values of λ.

In fact, in analogy to Table 2, Table 4, and Table 6 (for which $p=2$), Table 7, Table 8, and Table 9 contain analogous closed-loop nonlinearity bounds for $p=\infty$, thus correctly predicting the behavior of the peaks in Figure 11, Figure 13, and Figure 15.

The fact that closed-loop nonlinearity changes with the IMC filter time constant λ was also observed by Stack and Doyle (1997). However, these authors did not provide a means of predicting in which direction the nonlinearity would change (increase or decrease). The theory proposed in this work appears to provide such prediction, both qualitatively and quantitatively, thus aiding in controller design.

Example 7: Frequency Content of Nonlinear Closed-Loop Output. The nonlinear dynamic system in Example 1 is studied again to show the effect of a weighting function W on the bounds of $|W\Delta N|_{\Delta E2}$. Note that the operator W sees the difference between the outputs of the nonlinear and the linear closed loops $y_N - y_L$. Comparison between the results tabulated in Table 10 [for which $G_W(s)=1/(10s+1)$] and the results of Table 2 (for which $W=I$) shows that the low frequency contents of y_N and y_L do not differ. This is verified in Figure 19, which includes filtered responses for $G_W(s)=1/(0.1s+1)$, $G_W(s)=1/(10s+1)$, and $G_W(s)=1/(100s+1)$.

Conclusions and Discussion

In this work, we developed a theory and an associated computational methodology that address a basic question in controller design for nonlinear systems, namely "When and what linear control is sufficient for a nonlinear system". The theory is applicable to an extremely wide class of nonlinear processes. The basic result of this theory is Theorem 1, which introduces the important sets E and Z (to characterize the area of process operating conditions for which results are valid) as well as the quantities γ, α, and $\beta \triangleq \gamma/(1-\gamma)$. Using these concepts, Theorem 1 places bounds on an appropriately defined *closed-loop* nonlinearity measure. These bounds depend both on the nonlinearity of the controlled *nonlinear process* and on a *linear controller* guaranteed to stabilize that process. Computation of these bounds can be performed rigorously using Theorem 2, and approximations can be efficiently computed using Corollary 3, as described earlier. In addition to, and more importantly than its use as an analysis tool, the proposed approach can be used as a synthesis tool that enables the designer to easily design linear stabilizing controllers with predictable effects on closed-loop nonlinearity (hence, performance) for explicitly characterizable regions of process operation, without having to assume process oper-

Table 10. Lower and Upper Bounds of Closed-Loop Nonlinearity in Example 7 According to Theorem 1 and Corollary 3, for Different Values of λ in Eq. 78, $p=2$

			$\lambda=0.1$			$\lambda=1$			$\lambda=5{,}10$		
ϵ_S	y_s	u_s	$\eta_{\min}$	$\upsilon_{\max}$	γ_2	$\eta_{\min}$	$\upsilon_{\max}$	γ_2	$\eta_{\min}$	$\upsilon_{\max}$	γ_2
0	0	0	0	0	0	0	0	0	0	0	0
—	—	—	—	—	—	—	—	—	—	—	—
1.25×10^{-3}	1.4×10^{-3}	3.8896	0.073	0.4301	0.7096	0.0382	0.0697	0.2923	0.0377	0.0688	0.2923
1.50×10^{-3}	1.8×10^{-3}	4.6676	0.0859	3.6385	0.9538	0.0450	0.0964	0.3635	0.0444	0.0952	0.3635
1.75×10^{-3}			NA	NA	**1.2625**						
—			—	—		—	—	—	—	—	—
2.75×10^{-3}	3.7×10^{-3}	8.5572				0.0763	0.7715	0.82	0.0751	0.7592	0.82
3.00×10^{-3}	4.2×10^{-3}	9.3351				0.0821	2.6073	0.939	0.0807	2.5639	0.939
3.25×10^{-3}	4.7×10^{-3}	10.113				NA	NA	**1.3422**	NA	NA	**1.0710**

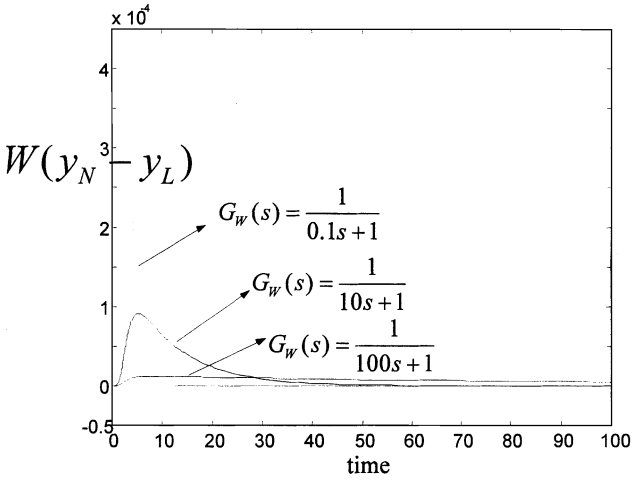

Figure 19. Filtered output differences $W(y_N\text{-}y_L)$ for different filters W.

Note that, for $G_W(s) = 1/(0.1s + 1)$, we obtain the same $y_N - y_L$ as in Figure 14.

ation near a steady state (needed for linear behavior). Process information needed by the proposed approach is multiple linear time-invariant process models, with each model being valid around a steady state within a range of process operation. Thus, the proposed theory and associated computational methodology also create a firm basis and establish novel ways for use of multiple linear models in linear controller design, an approach that has been repeatedly proposed by several authors on the basis of intuitive arguments. A number of examples earlier illustrate the usefulness of the proposed approach. In particular, predictions made by the proposed theory for several nonlinear systems are reliably verified by representative simulations.

It is clear that the proposed approach is only a first step towards understanding how nonlinear process dynamics and linear feedback interact. There are many potential extensions of the theory, as well as applications to specific classes of problems, a few of which are listed below.

- Establish tighter bounds for Theorem 1, if possible.
- Evaluate the accuracy of the approximation suggested by Corollary 3 for the computation of incremental norms over sets. Particular properties of the nonlinear process to be controlled, such as the lack of resonance frequencies or passivity, may prove useful. Moreover, the kind and amount of modeling information that can reliably answer whether linear control is sufficient for a nonlinear process is crucial from a practical viewpoint. For example, could steady-state information (readily available by commercial simulators) along with minimal information on process time constants be reliably used to determine adequacy of linear control?
- Characterize the sets E and Z more precisely. These sets refer to knowledge of the size of expected set point changes and disturbances, an issue independent of the particular controller used to control a given process. Disturbance estimates may be based on considerations similar to those taken into account during process design (such as, in order to size and temperature/pressure rate vessels, assign surge tanks, and so on) or standard controller design.
- Consider nonadditive disturbances.
- Evaluate the effects of model uncertainty.
- Examine the effects of initial conditions. Relevant work by Choi and Manousiouthakis (2000) and Sontag (2001) (in particular small-gain type of theorems) may prove useful.
- Examine the implications for constrained MPC. In particular, address the following practically important questions: "When and how can *constrained* MPC with *linear* model adequately control a *nonlinear* process?"
- Illustrate the proposed approach for multivariable processes.
- Examine the applicability of the proposed approach to nonlinear distributed-parameter processes. It is in principle conceivable that discretization of corresponding nonlinear partial differential equations can create nonlinear ordinary differential equations for which the proposed approach can be applied.

Acknowledgment

The authors gratefully acknowledge financial support from the National Science Foundation through Research Grant CTS-9615979.

Literature Cited

Allgöwer, F., "Definition and Computation of a Nonlinearity Measure," *Proc. of Nonlinear Control System Design Symp.*, NOLCOS95, Pergamon, Oxford, UK, p. 257 (1996).

Banerjee, A., Y. Arkun, B. Ogunnaike, and R. Pearson, "Estimation of Nonlinear Systems Using Linear Multiple Models," *AIChE J.*, **43**, 1204 (1997).

Cao, S. G., N. W. Rees, and G. Feng, "Analysis and Design for a Class of Complex Control Systems. 1. Fuzzy Modelling and Identification," *Automatica*, **33**, 1017 (1997).

Chen, C. L., S. H. Hsu, W. K. Lin, and T. C. Wang, "Identification of Multiple Linear Models for Nonlinear Processes," *J. Chin. Inst. Chem. Eng.*, **31**, 283 (2000).

Chen, H., A. Kremling, and F. Allgöwer, "Nonlinear Predictive Control of a Benchmark CSTR," *Proc. 3rd European Control Conf.*, ECC95, Rome, Italy (1995).

Chikkula, Y., J. H. Lee, and B. A. Ogunnaike, "Dynamically Scheduled MPC of Nonlinear Processes Using Hinging Hyperplane Models," *AIChE J.*, **44**, 2658 (1998).

Choi, J., and V. Manousiouthakis, "On a Measure of Bounded Input/Initial State Bounded Output Stability Over Ball," *Chem. Eng. Sci.*, **55**, 6059 (2000).

Desoer, C. A., and M. Vidyasagar, *Feedback Systems: Input-Output Properties*, Academic Press (1975).

Desoer, C. A., and Y.-T. Wang, "Foundations of Feedback Theory for Nonlinear Dynamical Systems," *IEEE Trans. Circ. Syst.*, Vol. CAS-27, 2, 104 (1980).

Dullerud, G. E., and F. Paganini, *A Course in Robust Control Theory: A Convex Approach*, Springer (2000).

Green, M., and J. N. Limebeer, *Linear Robust Control*, Prentice Hall, Englewood Cliffs, NJ (1995).

Guay, M., "Measurement of Nonlinearity in Chemical Process Control," PhD Thesis, Queen's University, Kingston, Ont., Canada (1996).

Guay, M., J. McLellan, and D. W. Bacon, "Measurement of Nonlinearity in Chemical Process Control Systems: the Steady State Map," *Can. J. Chem. Eng.*, **73**, 868 (1995).

Helbig, A., W. Marquardt, and F. Allgöwer, "Nonlinearity Measures: Definition, Computation and Applications," *J. of Process Control*, **10**, 113 (2000).

Helmicki, A., C. Jacobson, and C. Nett, "Identification in H_∞," *IEEE Trans. Auto. Contr.*, 1163 (1991).

Helmicki, A., C. Jacobson, and C. Nett, "Identification in H_∞," *IEEE Trans. Auto. Contr.*, 604 (1992).

Henson, M. A., and D. E. Seborg, "Input-Output Linearization of General Nonlinear Process," *AIChE J.*, **36**, 1753 (1990).

Johansen, T. A., and B. A. Foss, "Multiple Model Approaches to Modelling and Control," *Int. J. Control*, **72**, 575 (1999).

Morari, M., and E. Zafiriou, *Robust Process Control*, Prentice-Hall (1989).
Nikolaou, M., and V. Manousiouthakis, "A Hybrid Approach to Nonlinear System Stability and Performance," *AIChE J.*, **35**, 559 (1989).
Nikolaou, M., "When is Nonlinear Dynamic Modeling Necessary?," *Proc. of American Control Conf.*, San Francisco, CA, 1067 (Jun. 2–4, 1993).
Nikolaou, M., and V. Hanagandi, "Nonlinearity Quantification and its Application to Nonlinear System Identification," *Chem. Eng. Comm.*, 166, 1 (1998).
Nikolaou, M., "Computer-Aided Process Engineering in the Snack Food Industry," *Chem. Processes Control V*, AIChE Symposium Series, No. 93, 61 (1997).
Qin, S. J., and T. A. Badgwell, "An Overview of Industrial Model Predictive Control Technology," *Chemical Processes Control V*, AIChE Symp. Ser., No. 93, p. 232 (1997).
Qin, S. J., and T. A. Badgwell, "An Overview of Nonlinear Model Predictive Control Applications," F. Allgöwer and A. Zeng, eds., *Nonlinear Model Predictive Control*, Birkhauser, Switzerland (2000).
Rafal, M. D., and W. F. Stevens, "Discrete Dynamic Optimization Applied to On-Line Optimal Control," *AIChE J.*, **14**, 85 (1968).
Saaty, T. L., and J. Bram, *Nonlinear Mathematics*, McGraw-Hill, New York (1964).
Saaty, T. L., *Modern Nonlinear Equations*, McGraw-Hill, New York (1967).
Schrama, R., "Approximate Identification and Control Design," PhD Thesis, Dept. of Mech. Eng., Delft Univ. of Technology (1992).
Shinbroth, M., "Fixed Point Theorems," *Scientific Amer.* (Jan. 1966).
Skogestad, S., and I. Postlethwaite, *Multivariable Feedback Control: Analysis and Design*, Wiley, New York (1996).
Slotine, J. E., and W. Li, *Applied Nonlinear Control*, Prentice Hall, Englewood Cliffs, NJ (1991).
Sontag, E. D., "The Input to State Stability Philosophy as a Unifying Framework for Stability-Like Behavior," *Preprints of CPC VI Proc.* (2001).
Stack, A. J., and F. J. Doyle, "The Optimal Control Structure: an Approach to Measuring Control-Law Nonlinearity," *Computers Chem. Eng.*, **21**, 1009 (1997).
Stack, A. J., and F. J. Doyle, "Local Nonlinear Performance Assessment for Single-Controller Design," *IFAC World Congress* (1999).
Sun, D., and K. Kosanovich, "Nonlinearity Measures for a Class of SISO Nonlinear Systems," *Proc. of Amer. Control Conf.*, 2544 (1998).
Willems, J., *The Analysis of Feedback Systems*, MIT Press (1971).
Zhou, K., and J. C. Doyle, *Essentials of Robust Control*, Prentice Hall (1998).

Appendix A: Proof of Lemma 1

$\boxed{1. \Rightarrow 2.}$

Let $Tu_1 = Tu_2$ for two inputs u_1 and u_2 in U. Then $0 = \| Tu_1 - Tu_2 \| \geq c \| u_1 - u_2 \| \geq 0 \Rightarrow u_1 = u_2$ which implies that the inverse of T, T^{-1} exists. Next, consider any two elements $x_1 \neq x_2$ in X. Because T^{-1} exists, there exist u_1 and u_2 in U, such that $u_1 = T^{-1}x_1$ and $u_2 = T^{-1}x_2$. Therefore, by Eq. 15, $\| T(T^{-1}x_1) - T(T^{-1}x_2) \| \geq c \| T^{-1}x_1 - T^{-1}x_2 \| \Rightarrow \| T^{-1}x_1 - T^{-1}x_2 \| \leq 1/c \| x_1 - x_2 \| \Rightarrow \| T^{-1}x_1 - T^{-1}x_2 \| / \| x_1 - x_2 \| \leq 1/c$ for any two $x_1 \neq x_2$ in X. Taking the supremum over X yields $\| T^{-1} \|_{\Delta X} \leq 1/c < \infty$.

$\boxed{2. \Rightarrow 1.}$

Combination of the definition of the incremental norm of T^{-1} over the set X and Eq. 16 yields that

$$\left\| T^{-1}x_1 - T^{-1}x_2 \right\| \leq \left\| T^{-1} \right\|_{\Delta X} \| x_1 - x_2 \| \leq \frac{1}{c} \| x_1 - x_2 \|$$

for any $x_1 \neq x_2$ in X. Since x_1 and x_2 are images of elements u_1 and u_2 of the set U, the above equation implies

$$\left\| T^{-1}(Tu_1) - T^{-1}(Tu_2) \right\| \leq \frac{1}{c} \| Tu_1 - Tu_2 \| \Rightarrow \| Tu_1 - Tu_2 \| \geq c \| u_1 - u_2 \|$$

OEΔ.

Appendix B: Proof of Lemma 2

Consider any two elements u_1 and u_2 of the set U. Then

$$\begin{aligned} \| (I+R)u_1 - (I+R)u_2 \| &= \| u_1 + Ru_1 - u_2 - Ru_2 \| \\ &\geq \| u_1 - u_2 \| - \| Ru_1 - Ru_2 \| \\ &\geq \| u_1 - u_2 \| - \| R \|_{\Delta U} \| u_1 - u_2 \| \\ &= (1 - \| R \|_{\Delta U}) \| u_1 - u_2 \| \end{aligned}$$

By Eq. 17, we have that $1 - \| R \|_{\Delta U} > 0$. Consequently, the operator $T \triangleq I + R$ satisfies the conditions of Lemma 1 with $c \triangleq 1 - \| R \|_{\Delta U} > 0$. Therefore, $(I+R)^{-1}$ exists on Y, and is bounded as

$$\left\| (I+R)^{-1} \right\|_{\Delta Y} \leq \frac{1}{c} = \frac{1}{1 - \| R \|_{\Delta U}} < \infty$$

OEΔ.

Appendix C: Proof of Lemma 3

From Figure 1, we have

$$\begin{aligned} \epsilon &= r - [(w + d + NQ\epsilon) - LQ\epsilon] \\ &= r + LQ\epsilon - w - d + NQ\epsilon \\ &\Rightarrow (I + NQ - LQ)\epsilon = r - w - d \end{aligned}$$

If $(I + NQ - LQ)$ is invertible, then the above equation implies

$$\epsilon = (I + NQ - LQ)^{-1}(r - w - d).$$

Therefore,

$$y = d + NQ\epsilon = d + NQ(I + NQ - LQ)^{-1}(r - w - d).$$

OEΔ.

Appendix D: Proof of Corollary 1

$$\begin{aligned} y &= d + NQ(I + NQ - LQ)^{-1}(-d) \\ &= \left[-I + NQ(I + NQ - LQ)^{-1} \right](-d) \\ &= \left[-(I + NQ - LQ)(I + NQ - LQ)^{-1} \right. \\ &\qquad \left. + NQ(I + NQ - LQ)^{-1} \right](-d) \\ &= -(I - LQ)(I + NQ - LQ)^{-1}(-d) \end{aligned}$$

Equation 21 is trivial.
OEΔ.

Appendix E: Proof of Lemma 4

By definition

$$\Delta N \triangleq NQ(I+NQ-LQ)^{-1}-LQ$$
$$= NQ(I+NQ-LQ)^{-1} - LQ(I+NQ-LQ)(I+NQ-LQ)^{-1}$$

Because LQ is linear, the above equality yields

$$\Delta N = (NQ-LQ-LQNQ+LQLQ)(I+NQ-LQ)^{-1}$$
$$= ((I-LQ)NQ-(I-LQ)LQ)(I+NQ-LQ)^{-1}$$
$$= (I-LQ)(NQ-LQ)(I+NQ-LQ)^{-1}$$

OEΔ.

Appendix F: Proof of Lemma 5

$$NL^{-1}F(I+NL^{-1}F-F)^{-1}-F$$
$$= NL^{-1}F\left[I+(N-L)L^{-1}F\right]^{-1} - F\left[I+(N-L)L^{-1}F\right]\left[I+(N-L)L^{-1}F\right]^{-1}$$
$$= (NL^{-1}F-F-FNL^{-1}F+FF)\left[I+(N-L)L^{-1}F\right]^{-1}$$
$$= \left[(I-F)NL^{-1}F-(I-F)F\right]\left[I+(N-L)L^{-1}F\right]^{-1}$$
$$= (I-F)(N-L)L^{-1}F\left[I+(N-L)L^{-1}F\right]^{-1}$$

OEΔ.

Appendix G: Proof of Theorem 1

Direct application of Lemma 2 with $R \leftarrow NQ-LQ$, $U \leftarrow E$, and $Y \leftarrow Z \triangleq (I+NQ-LQ)(E)$ along with Eq. 35 in place of Eq. 17 implies that $(I+NQ-LQ)^{-1}$ exists on Z and is bounded as

$$\left\|(I+NQ-LQ)^{-1}\right\|_{\Delta Z} \le \frac{1}{1-\|NQ-LQ\|_{\Delta E}} \qquad (79)$$

which proves parts 1 and 2.

The equality in Eq. 36 has been proven in Lemma 4.

To establish the upper bound of $\|W\Delta N\|_{\Delta Z}$ in Eq. 36, we have

$$\|W\Delta N\|_{\Delta Z} = \left\|W(I-LQ)(NQ-LQ)(I+NQ-LQ)^{-1}\right\|_{\Delta Z}$$
$$\le \|W(I-LQ)(NQ-LQ)\|_{\Delta,(I+NQ-LQ)^{-1}(Z)} \left\|(I+NQ-LQ)^{-1}\right\|_{\Delta Z}$$

(because $\|AB\|_{\Delta X} \le \|A\|_{\Delta B(X)}\|B\|_{\Delta X}$ for any two operators A and B). Using Eq. 79 with the above inequality, we get

$$\|W\Delta N\|_{\Delta Z} \le \|W(I-LQ)(NQ-LQ)\|_{\Delta,(I+NQ-LQ)^{-1}(Z)} \times \frac{1}{1-\|NQ-LQ\|_{\Delta E}} = \frac{\|W(I-LQ)(NQ-LQ)\|_{\Delta E}}{1-\|NQ-LQ\|_{\Delta E}}$$

the last equality owing to Eq. 34.

To establish the lower bound of $\|W\Delta N\|_{\Delta Z}$ in Eq. 36, we apply the inequality

$$\|A\|_{\Delta X} = \|AB^{-1}B\|_{\Delta X} \le \|AB^{-1}\|_{\Delta B(X)}\|B\|_{\Delta X} \Rightarrow \|A\|_{\Delta X} / \|B\|_{\Delta X} \le \|AB^{-1}\|_{\Delta B(X)},$$

which immediately yields

$$\|W\Delta N\|_{\Delta Z} = \left\|W(I-LQ)(NQ-LQ)(I+NQ-LQ)^{-1}\right\|_{\Delta R} \ge \frac{\|W(I-LQ)(NQ-LQ)\|_{\Delta E}}{\|(I+NQ-LQ)\|_{\Delta E}}$$

OEΔ.

Appendix H: Proof of Corollary 2

Trivial by combining Eq. 36 with the inequalities

$$\|(I+NQ-LQ)\|_{\Delta E} \le 1+\|(N-L)Q\|_{\Delta E} \text{ and } \|W(I-LQ)(N-LQ)\|_{\Delta E} \le \|W(I-LQ)\|\|(N-LQ)\|_{\Delta E},$$

where the set over which the induced norm $\|W(I-LQ)\| = \|W(I-LQ)\|_{\Delta}$ is computed is irrelevant because the operator $W(I-LQ)$ is linear, OEΔ.

Manuscript received May 4, 2001, and revision received Jan. 15, 2002.